College of Engineering and Computing
DATA ANALYTICS ENGINEERING
George Mason University

Spring 2025

Post-Storm Flood Extent Shapefile Generation Using Satellite Imagery

DAEN 690

Project Report

Suhasini Manappa Chavan
Allison Forsyth
Santosh Kasula
Venkata Sai Nikhil Pasupuleti
Thomas Showalter
Rakesh Somukalahalli Venkatappa

About the Cover

This semester, the DAEN program is proud to spotlight one of our esteemed capstone partners, Daniel Erasmus—a visionary whose groundbreaking work influences leaders worldwide. As the founder and CEO of Erasmus.AI, Daniel is a renowned futurist and a pioneer in scenario planning, artificial intelligence, and strategic foresight. His innovative approach to blending AI with human-centric decision-making has profoundly shaped global conversations on technology, sustainability, and future-readiness. Through his thought leadership, Daniel continues to inspire organizations across the globe to embrace change and build resilient futures.

At Erasmus.AI, Daniel conceived and led the development of ClimateGPT—the world's first foundational AI model family focused on climate change. Built on over a decade of collecting and processing planetary-scale datasets, this groundbreaking innovation leverages AI to uncover hidden connections in global news, from Human-Centered Extreme Weather Dashboards to maps of global innovations, risks, and breakthroughs. The Erasmus.AI platform exemplifies his commitment to using technology to inform and address some of the world's most pressing challenges.

As co-founder of The Digital Thinking Network (DTN), Daniel has spent over 25 years leading large-scale scenario planning and transformation processes. His work has driven notable actions, such as initiating a response to food security challenges during COVID-19 that delivered 1 million meals within three months and has since provided over 60 million meals in Sub-Saharan Africa. His scenario processes have also anticipated major global events, including the Global Financial Crisis in 2006 and the Oil Price Collapse in 2012—each resulting in multi-billion-dollar benefits for his clients. In the public sector, DTN's transformative initiatives include the Rotterdam Advisory Board, which spearheaded the Rotterdam Climate Initiative in 2005 with the ambitious goal of halving CO2 emissions by 2025, and the creation of the 30-year global future scenarios Ci'Num.

An accomplished author, Daniel has written three books on innovation and the networked society, as well as numerous columns, including the Information Society column for the Financial Times Review. He has also held various prominent board positions and fellowships, including serving on the University of Stellenbosch's Faculty of Science Advisory Board, Cambridge-based Titan Advanced Energy Solutions, and the supervisory board of the Quad9 Foundation. Through his visionary leadership, Daniel continues to shape the future across disciplines and industries.

Contents

Table of Contents

Table of Figures

Table of Tables

This page intentionally left blank

Abstract

Abstract

Puerto Rico faces heightened flood risk due to its coastal geography and the intensifying effects of climate change, which have increased the frequency and severity of tropical storms and hurricanes. This project addresses the urgent need for accurate, near-real-time flood extent mapping to support disaster response efforts in flood-prone regions. This research focuses on generating post-storm flood extent shapefiles by leveraging Sentinel-1 (SAR) data, which offers cloud-penetrating capabilities, crucial for timely flood assessment. The project utilizes a combination of thresholding methods and conditional logic, including change detection, Otsu's adaptive thresholding, and VV/VH polarization ratio analysis to classify flood-affected regions. The processed data is then converted into GIS-compatible shapefiles for visualization in tools like QGIS and ArcGIS. Validation is conducted using historical flood records and data from the Global Flood Monitoring Portal. Findings demonstrate that automated SAR-based flood detection significantly enhances speed and accuracy in identifying flood extents compared to manual methods, making the approach ideal for supporting emergency response and resource allocation. By integrating these outputs into platforms like Arkly, the project delivers an accessible, user-friendly tool for disaster response teams and policymakers to assess real-time flood impacts and develop long-term resilience strategies. This research underscores the critical role of remote sensing and AI in addressing climate-related disasters and improving community preparedness in flood-prone regions.

This page intentionally left blank

Report

Section 1: Introduction

1.1 Report Purpose

The purpose of this report is to outline the analytics and techniques used to generate accurate post-storm flood extent shapefiles for disaster recovery efforts. The goals of this project include developing a pipeline to process satellite imagery for flood detection, generating shapefiles of the flood extent, and validating the flood extent shapefiles. The project will also create a user-friendly workflow for disaster response teams to access flood extent mapping post-disaster, which will enable teams to prioritize resources and aid. The subsequent sections of this report define the problem and solution space of post-flood disasters and flood detection, as well as the detailed methodology used to meet the project's outlined goals.

1.2 Report Readership

This report was conducted during a George Mason University capstone course for the Data Analytics Engineering department under the guidance of the Puerto Rico Science, Technology & Research Trust and HighTide AI. The report primarily targets the project partners in understanding how the team approached the proposed problem and details the algorithms and methods used to meet partner goals. Other target audiences include researchers in the fields of disaster recovery, data analytics, or GIS. The information in this report can be used to learn more about the connections between data analytics engineering and GIS, and how these fields can be applied to climate studies and disaster response methods, such as floods described in this paper.

1.3 Report Structure

The project report is outlined in 8 different sections, including the problem definition, datasets used for analysis and modeling, algorithms, testing and validation, findings, future work, and the final summary. The problem definition section describes the problem space for the project and research on previous studies in this space. It also covers the project objectives and user stories for the intended users of the product. The datasets section outlines the different datasets used for product development. The algorithms and testing sections detail the specific methodologies used to create the product and validate its use for end users. Lastly, the future work and summary capture the future ideas and possible research to be conducted based on the project findings. An appendix at the end of this report includes some domain background and a glossary of terms, as well as the team GitHub repository, project risks, agile development methods, and works cited.

Section 2: Problem Definition

2.1 Problem Space

The effects of climate change are leading to an increase in tropical storms, hurricanes, sea level rise, extreme heat waves, and other natural disasters. As a small island in the Caribbean, Puerto Rico is especially vulnerable to these effects due to its location and the coastal lowlands that surround the island. The island's geography, in combination with climate change impacts, puts Puerto Rico at a higher risk of experiencing floods.

In 2017, Hurricane Maria hit Puerto Rico, resulting in catastrophic wind and flood damage [1]. The category 5 hurricane dropped over 20 inches of rain in some areas of Puerto Rico, with winds over 100 miles per hour [2]. The intensity and volume of rain and wind amplified the impact of the hurricane on the community, taking the lives of almost 3,000 people and resulting in an estimated $90 billion economic loss [1]. More recently, Hurricane Ernesto hit Puerto Rico in 2024, again bringing heavy winds and nearly 10 inches of rainfall [3]. The category 1 hurricane caused severe flooding and power outages on the island.

Figure 1: Image from Bloomberg: Hurricane Ernesto

Climate change is continuing to amplify the frequency and intensity of tropical storms, which will likely come with increased precipitation and increased coastal storm surges [1]. The stronger storms will amplify current flood risks in Puerto Rico's communities that are already being impacted. In addition to its vulnerability to tropical storms, Puerto Rico also faces the effects of sea level rise from climate change, increasing the flood risk to coastal neighborhoods. Since records of sea level began in 1880, Puerto Rico's sea level has risen 6 feet [4]. Due to climate

change, the rate of sea level rise has accelerated, with scientists projecting 22 inches by 2060 [4]. The change in sea level will likely heighten the flooding from major storms in the future.

The effects of climate change, particularly the increased frequency and strength of tropical storms and sea level rise, place Puerto Rico at an even greater risk of floods that have a direct effect on the community. It's important for the communities of Puerto Rico to understand their flood risk, as it is the leading cause of death and property damage following a large tropical storm event [1]. Current flood risk mapping, powered by HighTide AI, allows Puerto Rico communities to better understand their flood risk [5]. Their model quantifies the impacts of a flood event in risk zones by dollars and the number of people at risk [5]. Tools such as Arkly, powered by HighTide AI, and FEMA flood risk maps enable communities to learn and adapt to become more flood-resilient. Flooding is attributed to being one of the most expensive and damaging natural disasters, so understanding flood risk early allows for proactive intervention methods such as building flood-resilient architecture in at-risk communities [5].

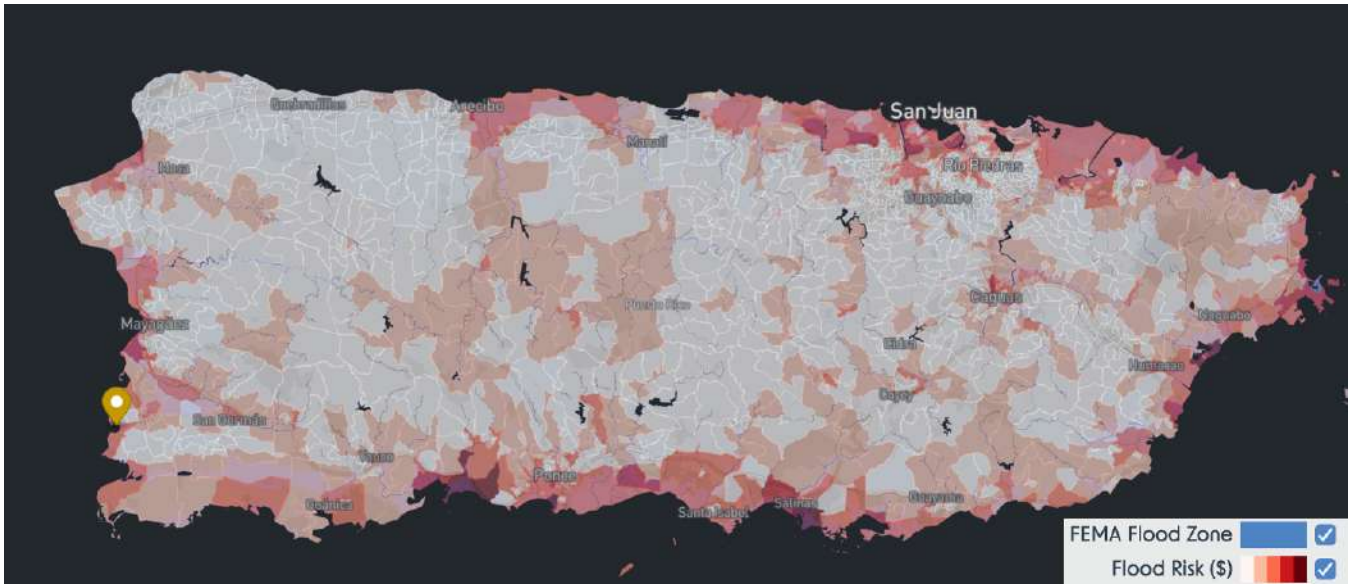

Figure 2: Hightide AI Arkly Platform Map

Our primary sponsor for this project, the Puerto Rico Science Technology and Research Trust, operates the Caribbean Center for Rising Seas, which also partners with Hightide AI to focus on community resilience and adaptation for flood risk areas [6]. Their main mission is to prepare Puerto Rico and the surrounding Caribbean islands for the increasing flood risks due to climate change, providing education, outreach, and best practices for flood-resilient communities [6]. Their current solutions include Safe Advance Flood Estimates (SAFE) to guide coastal design, planning, and engineering, working with architecture, engineering, finance, and legal environment professionals to educate and provide resources, establishing policies for building codes and zoning, and community outreach efforts [6]. These solutions benefit Puerto Rico by increasing flood resiliency, decreasing flood damage, and mitigating loss of life [6]. The Caribbean Center for Rising Seas and its proactive approach to flood risk allow affected communities to thrive when faced with increased floods, hurricanes, and rising sea levels.

While current methods exist for evaluating community flood risk and the economic impact of flooding, there is no method for near-real-time flood extent mapping in Puerto Rico. Mapping floodwater extent is crucial to disaster recovery efforts post-storm surges to aid in identifying the areas of greatest impact and allocate resources effectively. In combination with its flood resiliency efforts, Puerto Rico can use near-real-time flood extent

mapping to assess the magnitude of a live flooding event and help assess damage. It can also help identify communities with a greater need for flood-resilient intervention post-flood. Successful flood extent mapping will not only drive effective post-storm disaster recovery efforts but also aid in the ongoing efforts of assessing flood risk and driving resilient communities.

2.2 Research

The first stage of research that the team undertook for this project had two primary objectives. One of these objectives was to gain a preliminary understanding of the project space beyond the scope of what was covered during the weekly sponsor meetings. The other objective was to begin to understand possible solution paths for the project and to gain an understanding of solution paths used to solve similar problems in the past by others. The purpose of performing such research during the early stages of the project is to allow future decisions made by the team to be as informed as possible and, ideally, to recognize and avoid some of the same mistakes made by others who have worked to solve similar problems in the past.

Satellite Image Research

First, the team gathered information on possible data sets from researching satellite images. It's important to understand the various satellites and image types available from those satellites, as they will be our primary source of data in detecting floods. The team started by looking at two satellite imagery sources with open user access: NASA's Landsat satellites and Copernicus Sentinel satellites.

NASA Landsat Missions:

NASA's Landsat satellites provide optical imagery of Earth's land surface. The data from Landsat satellites is distributed by the United States Geological Survey Earth Resources Observation and Science Center. Landsat Collection 2 data contain Level-1, Level-2, and Level-3 image products from contributing Landsat Missions. Level-1 products are preprocessed in various ways determined by the existence of ground control points, elevation, and payload correction from the sensor. These images contain calibrated digital scale numbers representing the multispectral image data. Within Level-1, products can either be tier 1 or tier 2, depending on data quality and terrain precision. Tier 1 images contain the highest available data quality with "well-characterized" radiometry and inter-calibration across other Landsat satellites. While tier 2 images meet the same radiometric standards as tier 1, they tend to have less accurate orbital information, making geometry less specific, or contain significant cloud cover. Landsat Level-2 and Level-3 products contain time-series observational data to measure the effects of environmental change. Products in these levels include surface reflectance, surface temperature, burned area, dynamic surface water extent, and more. Dynamic surface water extent, which may be useful for flood detection, describes the existence and condition of surface water. [7]

While Landsat optical image products like dynamic surface water extent may be useful in developing post-storm flood extent boundaries, the image data is unable to penetrate clouds. The ability to obtain cloud-free satellite image data is important in post-storm flood detection, as many post-storm optical images contain clouds, which would make groundwater detection more difficult.

Copernicus Sentinel:

Similar to NASA's Landsat Missions, the European Space Agency's Earth Observation component, Copernicus, has several Sentinel Missions that capture different satellite images [8]. For our research, we focused on Sentinel-1 and Sentinel-2 missions. Like the NASA Landsat missions, Sentinel-2 takes optical images of Earth's surface. The mission contains two polar-orbiting satellites aimed at monitoring Earth's surface changes [8]. Sentinel-2 has several products similar to NASA's Landsat products, including surface reflectance images, satellite image mosaics,

and more [8]. The Sentinel-1 mission also contains two polar-orbiting satellites that use C-band Synthetic Aperture Radar (SAR) imaging. SAR imaging allows Sentinel-1 to capture images in any weather condition, making it optimal for post-storm flood extent detection [8]. SAR imagery works by sending out pulses of energy and recording the amount of energy reflected back to the satellite from the Earth's surface [9]. The satellite radar instruments use longer wavelengths that allow them to penetrate clouds or tree canopies to retrieve a more accurate surface image [9]. The surface image collections from Sentinel-1 include Level 1 ground Range Detected (GRD), Level 1 Single Look Complex, Level 2 Ocean, and more [8]. GRD products contain ground range coordinates with pixel values representing detected amplitude from the satellite wavelengths [8]. The primary acquisition mode of Sentinel-1 is Interferometric Wide Swath (IW), which uses dual or single polarization to create bands, or swaths, that are merged to create the full image product [8]. Polarization refers to the "orientation of the plane in which a transmitted wave oscillates" [9]. These signals are characterized by an "H" or "V" depending on horizontal or vertical polarization [9]. Signals can be emitted and received in different polarizations, denoted by "VV" for vertical send and receive or "VH" for vertical send and horizontal receive, for example. The signal strengths in each polarization can also give valuable surface information, depending on a rough surface, volume, or double-bounce scatter [9]. For example, rough surface scatter, most sensitive in VV images, can be caused by energy waves hitting bare soil or water [9]. Sentinel-1 data products are also preprocessed to adjust backscatter denoted by "gamma0" [8]. The gamma0 correction reduces the impact of the changes due to the satellite angle, normalizing the backscatter and providing consistent measurements across different satellite image angles [8]. Due to its ability to penetrate clouds, the difference in pixel values from water to land, and multiple polarizations, SAR imagery is optimal for use in detecting floods or changes in water extent on the Earth's surface [8].

Flood Detection Method Research

Flooding is one of the most catastrophic natural disasters, affecting infrastructure, crops, and human life. Accurate and fast flood mapping is critical for disaster response and mitigation. Traditional flood detection approaches use optical remote sensing (e.g., Landsat, Sentinel-2) and SAR-based thresholding techniques.

However, based on our research and knowledge, machine learning (ML) and deep learning (DL) models give a more advanced and automated method, enhancing accuracy and flexibility [10]. Our research focuses on AI/ML-driven flood detection in Puerto Rico utilizing Sentinel-1 SAR data, namely the VV and VH polarization bands. This project seeks to construct an efficient and effective flood detection pipeline that includes SAR image processing, AI-based classification, and GIS mapping.

Our research focuses on detecting floodwater using Sentinel-1 SAR imagery. The study explores advanced methodologies, including:

Change Detection

Change detection entails comparing pre- and post-flood Sentinel-1 SAR images to detect differences in water coverage. Floodwater-affected locations can be recognized and classified using established parameters by calculating the difference in backscatter intensity[11]. This approach effectively captures quick changes in water extent and can be further refined utilizing AI-driven models, which help refine classification accuracy by learning complicated spatial patterns and decreasing misclassifications. Various AI techniques are being researched to establish the best model for this application.

Unsupervised Learning

Unsupervised learning techniques classify floodwater by identifying patterns in SAR backscatter intensities without requiring labeled training data. These methods rely on statistical similarities and clustering algorithms to differentiate water-covered areas from non-water regions. Several techniques, including clustering-based,

probabilistic, and neural network-based approaches, are being considered for their ability to generalize across varying flood conditions. Additionally, feature extraction methods such as Autoencoders and Self-Organizing Maps (SOMs) may improve classification accuracy by learning intrinsic patterns in SAR data. The evaluation of different unsupervised techniques is ongoing to determine the most effective approach for floodwater detection.

Histogram Thresholding

Histogram thresholding is a popular approach for separating floodwater based on SAR backscatter intensity distributions. Using a histogram of backscatter measurements, water reflectance levels can be identified and used for segmentation. Statistical thresholding methods, such as Otsu's Method, aid in distinguishing floodwater from non-water regions, resulting in a binary flood mask for subsequent GIS processing. Adaptive ML-based thresholding approaches, such as Random Forest classifiers and Bayesian Thresholding, can dynamically alter thresholds based on contextual data, leading to improved accuracy. Continuous studies are being carried out to establish the most efficient thresholding strategy for flood detection.

Supervised Learning (AI & ML models):

Supervised learning techniques use labeled SAR flood datasets to train models that can accurately classify pixels. These models use known floodwater properties to distinguish water from non-water locations, increasing detection accuracy.

Various machine learning and deep learning models are being investigated, however, the specific technique to be employed is still being evaluated. Traditional machine learning classifiers like Random Forest (RF) and Support Vector Machines (SVM) are being studied alongside more advanced deep learning models, including Convolutional Neural Networks (CNNs) and U-Net segmentation networks[12].

Transformer-based architectures, such as Swin-Transformer, are being evaluated for their capacity to detect spatial dependencies in SAR pictures (12). The ultimate strategy will be chosen based on comparative evaluations of accuracy, computing efficiency, and floodwater detection application in the real world.

2.3 Solution Space

Based on research into the problem space and data available, we will use unlabeled data from pre- and post-flood satellite images and use change detection methods to identify areas of potential flooding. The change detection classification algorithm will detect the changes in pixel layer values and, based on a certain threshold, will classify a pixel at a certain latitude and longitude as being flooded. Using this method will allow us to classify pre-flood water and post-flood water using research-backed decibel threshold values. Building off the original flood classification model, the team will further refine the flood extent using several logic-based conditions based on flood research, such as the area of a flood and slope. The system will drive value to users as they will be able to classify flooded areas in near real-time with access to satellite images. In addition to classifying flooded areas, our solution will provide a shapefile image and map of the flooded areas for use in disaster response. The shape file and map of the flood extent will be easily readable by users to gain a better understanding of which neighborhoods or towns are the most affected in an effort to help prioritize resources where they are most needed.

2.4 Project Objectives

Four key objectives were provided by the Puerto Rico Science, Technology & Research Trust for post-storm flood extent mapping.

1. Develop a pipeline to process satellite imagery for flood detection: Using available satellite images, the team will develop a pipeline in Python that will ingest pre- and post-flood satellite data and run it through a machine learning model that will classify areas in the image that have flooded.
2. Generate GIS-compatible flood extent shapefiles: After completion of the classification algorithm, we need to use the latitude and longitude coordinates from flooded areas to compose a GIS-compatible shape file. The team will also provide GIS mapping visuals of the flood extent for easy readability by users.
3. Evaluate accuracy against ground-truth data where available: Evaluate the accuracy of the proposed classification algorithm using historical flood information. As the model is fed using unlabeled satellite imagery, we need to ensure the accuracy of the model by testing it on previous floods not used in model training.
4. Create a user-friendly workflow for disaster response teams: Create a user-friendly workflow that disaster response teams will be able to follow and understand when needing to map flood extent. The workflow and solution should be able to be used by anyone, no matter their knowledge of satellite images or GIS tools.

Driven by the outlined objectives, the team will learn how to process and read satellite images and how to use the underlying data within those images to build a classification algorithm. The team will also gain a better understanding of the types of data collected from different satellite images and the degree to which the values of data change from pre-flood to post-flood images. From building our understanding of the primary data sources, satellite images, the team hopes to achieve a highly accurate classification model that will drive greater efficiency and resource allocation in flood disaster response for Puerto Rico.

2.5 Primary User Stories

As a disaster response team, we want a user-friendly workflow that will enable us to see up-to-date, real-time flood extent boundaries that will allow us to prioritize resources and aid to flooded communities. We want an accurate flood extent map that will provide information about the affected communities and help us understand the magnitude of the flood event so we can mitigate damage.

2.6 Product Vision

2.6.1 Scenario #1

Disaster response teams will be able to use the product from this project to help map flood extent after a flooding event. The product will be able to quickly evaluate changes in satellite image data to determine specific geographic locations that have flooded. Unlike current methods, this product will be able to provide near real-time information, providing shapefiles and GIS maps to easily locate the communities affected. This will allow a better allocation of resources to the communities in the most need.

2.6.2 Scenario #2

Policymakers involved in disaster recovery or climate areas may be able to use this product to track flood extent after floods to get a better understanding of flood risk areas. As climate change continues to have a lasting effect on Puerto Rico, this will allow policymakers to track flood extent changes in towns and neighborhoods after major flood events. The ability to understand the change in flood extent over time will allow policymakers to advocate for resources and infrastructure to enable Puerto Rico to be more resilient against floods in high-risk areas.

Section 3: Datasets

3.1 Overview

The primary data sources for this project include multiple satellite images accessed from the Copernicus Sentinel satellites from the European Space Agency. Each visual layer contains different data for pixels, defined by their longitude and latitude, that can be used in flood detection by measuring the change in pixel value from pre-flood and post-flood satellite images. Several data layers of the Sentinel-1 images are available, including the following:

VH Decibel gamma0:
VH decibel Gamma0 is a grayscale visualization of the gamma0 of VH polarization. This image shows the decibel values of each pixel in grayscale, where lower values indicate lower reflectance (water), and higher values indicate more reflectance of the satellite wavelengths (land). The measured decibel values are calculated by performing a logarithmic scaling of the returned satellite image data.

VV Decibel gamma0:
Similar to the VH decibel gamma0, VV decibel Gamma0 is a grayscale visualization of gamma0 of the VV polarization with the same data interpretation. Unlike VH polarization, the VV band is more sensitive to surface roughness compared to VH.

RGB ratio:
RGB (red, green, blue) ratio is a combination of gamma0 and VV and VH polarization that creates a false color visualization. The VV polarization creates the red band, VH polarization the green band, and a combination of VV/VH creates the blue band.

Enhanced visualization:
The enhanced visualization combines gamma0, VV, and VH polarization to create a false-color image of the data. This layer primarily contains blue and green values, where blue indicates water and a combination of yellow and green represents land.

To narrow the size of our data and from previous research on flood detection, the team will focus on data collection and interpretation from VH and VV decibel gamma0 layers. These grayscale images provide VV and VH decibel values on a scale from 0-255. While these gray-scale images help provide visual interpretations of decibel values, the team needed the actual decibel values, which are normally interpreted on a scale from 0 to -20. Exploring the Copernicus Ecosystem, the team was able to extract exact decibel values with backscattering and speckle filtering applied to use in algorithm development.

The data was collected by using the Copernicus Process API, which allows users to access satellite image data directly from their code base. Within the Process API, we specify the image layer, time scope, image properties, and data preprocessing or cleansing steps. More information on the Process API and image specifications can be found in section 3.3 Data Context.

3.2 Field Descriptions

As described above, our primary data is gathered from Sentinel-1 SAR imagery data, particularly the VV and VH Decibel Gamma0 layers. The raw image data fields are listed in the table below.

VH Decibel Gamma0 (visual)		
Band 1	Type: Integer	"red" band value containing number between 0-255 representing the VH decibel value
Band 2	Type: Integer	"blue" band value containing number between 0-255 representing the VH decibel value
Band 3	Type: Integer	"green" band value containing number between 0-255 representing the VH decibel value
Band 4	Type: Integer	Data mask which contains 0 for no data and 1 for data
VH Decibel Gamma0 (decibel values)		
Band 1	Type: Integer	Decibel value containing number between 0 and ~-22
VV Decibel Gamma0 (visual)		
Band 1	Type: Integer	"red" band value containing number between 0-255 representing the VH decibel value
Band 2	Type: Integer	"blue" band value containing number between 0-255 representing the VH decibel value
Band 3	Type: Integer	"green" band value containing number between 0-255 representing the VH decibel value
Band 4	Type: Integer	Data mask which contains 0 for no data and 1 for data
VV Decibel Gamma0 (decibel values)		
Band 1	Type: Integer	Decibel value containing number between 0 and ~ -22

In addition to the data fields listed above, the following GeoTIFF file information is available.

Category	**Field**	**Type**	**Description**
Image Data Fields (Raster Properties)	Width	Integer	Number of pixels in the x-direction (columns)
	Height	Integer	Number of pixels in the y-direction (rows)
	Count	Integer	Number of spectral bands
	Dtypes	List of strings	Data type of the pixel values
	Driver	String	File format
	Nodata	Float or None	Value representing missing data (if any)
	Compression	String or None	Compression method (if any)
Spatial Reference System Fields (CRS)	Crs	CRS object	Coordinate reference system (CRS)
	Transform	Affine object	Affine transformation matrix, maps pixel coordinates to real-world coordinates
	Bounds	BoundingBox object (tuple)	Bounding box, geographic extent of the image

	Res	Tuple (float,float)	Pixel size in real-world units
Metadata Fields	Meta	Dictionary	Dictionary containing key metadata attributes
	Tags()	Dictionary	Custom metadata stored in file
	Overviews	List of integers	List of overview levels (if pyramids exist)
	Interleave	String	Data organization (band-sequential or band-interleaved)
Band-Specific Information Fields	Read	Numpy array	extracts band i as a numpy array
	ColorInterp	ColorInterp object	color interpretation of band i
	Mask_flag_enums	List	mask flags for band i

3.3 Data Context

The data used in our initial research was focused on Hurricane Maria, which hit Puerto Rico in September 2017. We used the Copernicus Process API to gather pre- and post-flood image data from a small portion of the northeast side of the island. All primary data was gathered from the ESA Sentinel-1 mission. For our area of interest (AOI), we specified a range of dates from which to create mosaics; these mosaics gather all image data available from the selected date range and, where data is available, combines the data into one satellite GeoTIFF. Hurricane Maria made landfall in Puerto Rico on September 20^{th,} so our pre-flood date range was selected from September 1, 2017, to September 16, 2017, and our post-flood date range from September 20, 2017, to September 28, 2017.

To better understand the decibel values pre- and post-flood, 3 pre-flood images were captured, and 2 post-flood images were captured within the specified dates above. This method of data collection allowed the team to calculate mean values with pre- and post-flood decibel values rather the relying on a single pre- or post-flood image for flood classification. This was especially important with pre-flood images, as day-to-day decibel values can vary and may cause inaccuracies in flood classification.

Due to the data download capacity and resolution limits with the API, we separated the AOI into a 5-cell grid where we pulled pre- and post-flood VV and VH decibel values (both VV and VH were pulled in the same GeoTIFF), resulting in 25 separate GeoTIFFs (3 pre-flood, 2 post-flood) that were later combined to create the entire AOI image. Within the satellite image data, each data point represents a 10x10 meter pixel, the highest resolution available. Figures 3 and 4 below depict the complete pre- and post-flood VH images covering our AOI.

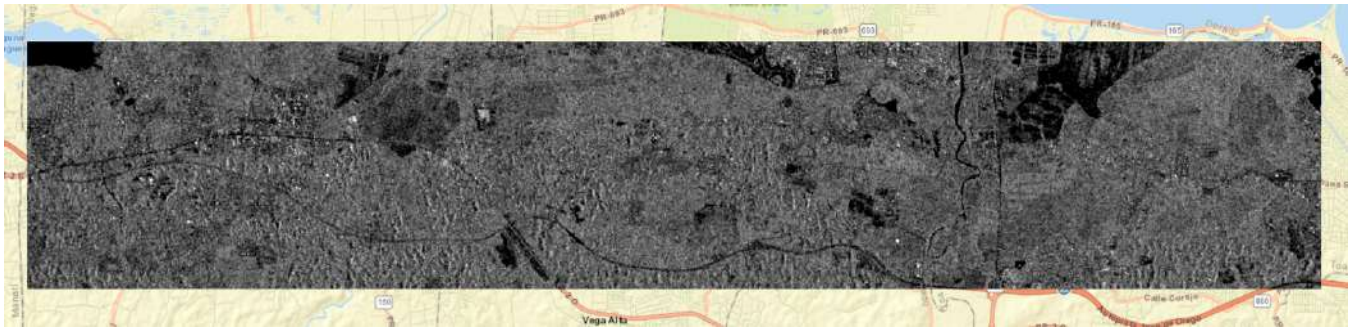

Figure 3: Pre-Flood VH Image

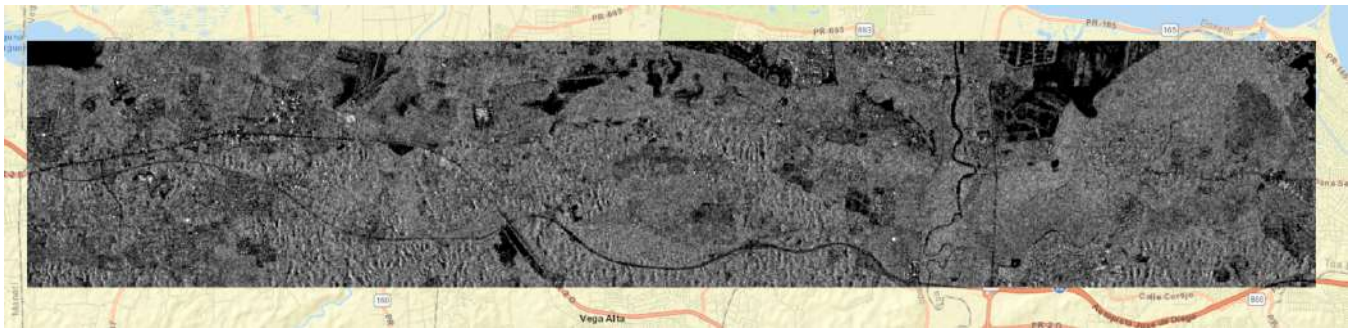

Figure 4: Post-Flood VH Image

Interferometric Wide Swath mode was selected as the satellite acquisition mode in the API as it is the most commonly used and default acquisition mode; more details on Interferometric Wide Swath can be read in the satellite image research portion of the paper. In addition to the VV and VH layer specification and date range selection, several data conditioning steps were applied when downloading data from the API. These data conditioning steps include a backscatter coefficient, speckle filtering, and orthorectification. These steps are described in more detail below.

3.4 Data Conditioning

To clean the satellite image data and correct any image distortions, a backscatter coefficient, speckle filter, and orthorectification were applied through the Process API download. A backscatter coefficient measures how much a wavelength from the satellite is scattered by the Earth's surface. The coefficient is applied to the data to correct any backscatter errors from the image caused by geometric and radiometric distortions. For our data collection, the gamma0 terrain backscatter coefficient was selected to correct the backscatter for the effects of the surrounding terrain, meaning the resulting image can be interpreted as if the image were flat and disregarding topography effects. The applied speckle filter cleansing step improves image quality by reducing granular noise caused by the interference of wavelengths from the satellite. The final data cleansing step in the Process API is applying orthorectification, set to "TRUE", which corrects any image distortions from the angle of the satellite sensor system.

3.5 Data Quality Assessment

The Sentinel-1 dataset provides a high-resolution and structured source for flood detection, ensuring precision and reliability in analytical workflows. Data retrieval through the Copernicus Process API maintains consistency across acquisitions, allowing seamless integration into geospatial frameworks. With a spatial resolution of 10x10 meters per pixel, each image captures fine-scale variations in reflectance, essential for detecting changes in water accumulation. The ability to compare pre- and post-flood conditions using Gamma0 VH and VV decibel layers ensures that surface changes are both measurable and accurately represented, reducing uncertainties in flood extent estimation.

Preprocessing steps refine the dataset by correcting terrain distortions and sensor-induced anomalies. The Gamma0 terrain backscatter coefficient adjusts radar reflectance values to align with actual surface properties, while orthorectification ensures spatial accuracy by aligning images to true geographic coordinates. These corrections prevent misalignment issues and enhance the reliability of multi-temporal analysis. Speckle filtering further improves image clarity by minimizing granular noise, a common artifact in SAR imagery.

Each GeoTIFF file contains discrete spectral bands (VV and VH decibel gamma0), preserving independent yet complementary flood indicators. Rescaling decibel values to a 0-255 grayscale format standardizes the representation across datasets, allowing direct integration into GIS applications without additional transformation. The structured organization of bands, where red, green, and blue channels retain identical values, ensures that pixel data remains intact while facilitating visual interpretation. This separation of image components supports analytical models in leveraging the most relevant spectral responses without interference.

The dataset structure aligns with Copernicus Sentinel-1 protocols, with metadata fields such as the coordinate reference system (CRS), affine transformation matrix, and bounding box definitions embedded within each file. This standardization simplifies integration with auxiliary geospatial datasets and supports automated processing pipelines where consistency is key.

The Area of Interest (AOI) is divided into 25 GeoTIFFs, ensuring comprehensive spatial coverage of flood-affected regions. With both pre-flood and post-flood acquisitions, the dataset enables a comparative approach to analyzing water distribution changes over time. Metadata elements such as overview levels, interleave structure, and compression parameters streamline storage and retrieval, optimizing performance without compromising data integrity.

The Sentinel-1 dataset is well-suited for flood analysis, balancing precision, structural consistency, and processing efficiency. Its high spatial resolution, standardized radiometric corrections, and metadata-rich format contribute to a reliable dataset that scales effectively for large-area assessments. By maintaining a structured approach to data acquisition, processing, and storage, it remains a valuable resource for flood detection and geospatial analysis.

3.6 Other Data Sources

One additional data source that was consulted was data from the GloFAS Global Flood Monitoring (GFM) portal. This data source is made available by the Copernicus Emergency Management Service and is generated in near real-time using Sentinel-1 SAR imagery. The GFM data provides eleven different layers related to flood detection, eight of which can be downloaded in a raster (GeoTIFF) format. Of these layers, the layer likely to be of greatest interest to this project is the first layer, which identifies the observed flood extent. Other layers map features such as the observed water extent, a reference water mask, an exclusion mask, and an uncertainty mask, among others.

The GFM flood extent data is generated through a combination of three algorithms. These include a logistic-based image segmentation and thresholding (LIST) algorithm, a DLR flood mapping algorithm, and a TUW flood mapping algorithm. If two of the three algorithms detect flooding in a given unit, then the GFM data indicates positive for flooding. The algorithms used to generate the GFM data provide possible avenues to explore for developing a flood detection algorithm for this project. Additionally, the GFM data provides a useful set of baseline data for evaluating the performance of various flood detection algorithms and identifying flooded areas that could be used to train algorithms.

In addition to the GFM flood extent, we used aerial images collected from the National Oceanic and Atmospheric Administration for flood validation. A team of NOAA aviators took these aerial images 2-4 days after Hurricane Maria, using specialized cameras from 500-1500 meters above the surface. Due to other possible validation data sets using similar techniques and algorithms, this aerial imagery is the best source of ground truth data.

3.7 Storage Medium

The data from the Copernicus browser system is retrieved through an API call and stored in a personalized repository, where we code and execute commands in Python. All this information is then stored in a shared GitHub repository, accessible to the development team.

Each team member accesses the repository, updates their code, and uploads the results generated from running and testing the scripts. Other storage options for outputs and generated information include local storage on laptops or PCs used to run the codes and algorithms planned in the repository. To ensure no data is lost, results are regularly uploaded to GitHub for backup and collaboration.

Exploring cloud-based storage options or even utilizing a potential built-in storage system within the Arkly website, if available, would be a significant step forward. This would allow for the efficient handling of vast amounts of data, ensuring better accessibility and scalability for deploying query results in the next stage of development.

3.8 Storage Security

All Sentinel-1 data utilized in this project is publicly available and freely accessible, eliminating the need for strict security measures. Since the data does not contain sensitive or proprietary information, encryption or restricted access protocols are not required. The GitHub repository serves as a collaborative platform where all team members can freely access and update code and processed datasets. Local storage on individual machines is used primarily for temporary processing, and since no confidential data is involved, security concerns remain minimal.

However, while the data itself is public, access to stored and processed results, scripts, and workflow files in the GitHub repository should ideally be limited to team members or relevant stakeholders to prevent unauthorized modifications or accidental data loss. Ensuring that only authorized contributors have written access can help maintain the integrity of the project. Additionally, while local storage does not pose significant security risks, data corruption, accidental deletions, or hardware failures could still impact workflow efficiency, highlighting the need for routine backups. If the project scales to incorporate larger datasets or integrates additional private resources, future security measures such as controlled access permissions, versioning, and off-site backups may need to be considered.

3.9 Storage Costs

GitHub serves as a cost-effective storage solution for project development since it does not incur additional costs for storing code, scripts, and smaller datasets. However, as the data size increases, particularly with large satellite imagery and processed outputs, storage limitations may become a concern. While local storage on individual machines can handle temporary data, it is not ideal for long-term scalability. Exploring cloud-based solutions or a dedicated in-house storage system would provide a more structured approach to managing large datasets despite potential cost implications. Even if costs rise, investing in scalable and efficient storage options could be beneficial in ensuring seamless data access, processing, and deployment for future developments.

Section 4: Flood Extent Algorithms and Analysis

4.1 Algorithms and Analysis

The algorithms and analysis walk through the steps taken to create our final proposed flood extent shape file. First, we explain the several methods chosen through research and testing that led to the flood extent, such as change detection, thresholding, and refinement. Next, we walk through the use of the proposed algorithms using our area of interest described in section 3.1.

4.1.1 Algorithms

Change Detection:

Change detection is a widely used technique in flood detection, especially with Synthetic Aperture Radar (SAR) imagery. It involves comparing pre-event and post-event images to identify differences caused by flooding. The process relies on analyzing changes in the backscatter values (in decibels, dB) between two sets of images — one or multiple taken before the flood and one or multiple taken after the flood.

For this project, Sentinel-1 SAR images from the Copernicus Data Space Ecosystem are being used. The main steps involved in change detection include:

- Preprocessing of Sentinel-1 data (radiometric and geometric corrections)
- Conversion of backscatter values into dB using the equation:

$$x_{dB} = 10log_{10}(x)$$

  Where x is the pixel value
- Comparison of pre-flood and post-flood dB values to identify areas where a significant decrease in backscatter is observed, which indicates the possible presence of water.

Thresholding:

Thresholding is a method used to classify flooded and non-flooded areas based on backscatter intensity. In SAR imagery, water surfaces usually appear darker due to low backscatter caused by the smoothness of water surfaces.

Thresholding involves setting a dB value to separate water from non-water surfaces:

- Water surfaces generally have backscatter values between -22 dB and -18 dB.
- Partially flooded and vegetated areas range from -18 dB to -16 dB.
- Urban and dry land surfaces have higher backscatter values above -16 dB.

For this project, thresholding at -16dB, -18 dB, and -20 dB was used as an initial classification method to distinguish flooded areas from non-flooded areas. While previous research and widely accepted thresholds for water presence exist, we further refine the threshold using Otsu's method.

Otsu's Method for Adaptive Thresholding:

Otsu's method is an automated thresholding technique that determines the optimal threshold value by minimizing the variance within the thresholded classes. This technique will help in:

- Identifying an adaptive threshold for separating water from non-water surfaces.

- Improving classification accuracy in areas with mixed land cover (e.g., urban areas with partially flooded roads).

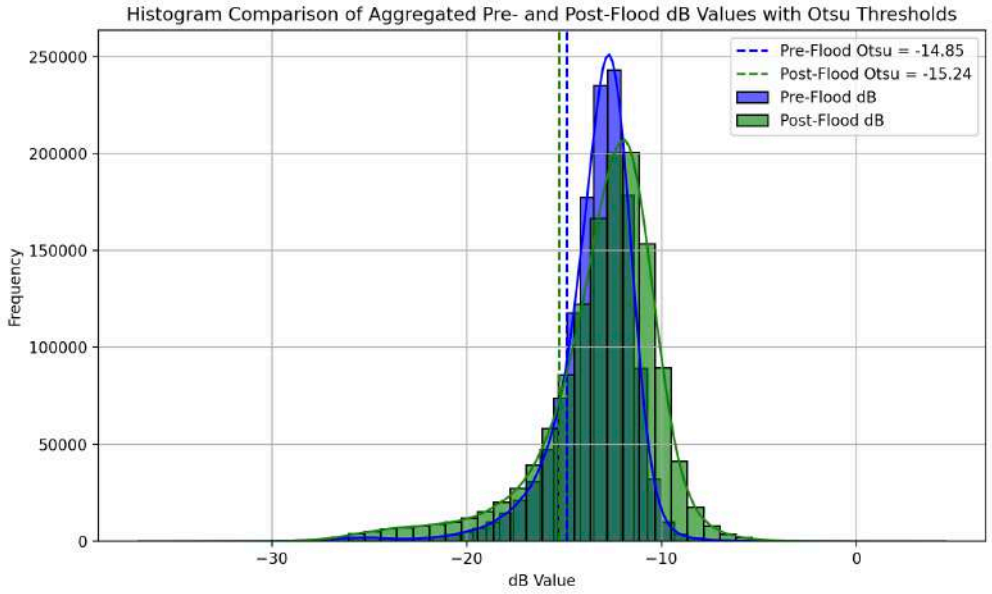

Figure 5: Otsu's Method on AOI1

Given the minimal difference in the adaptive threshold, thresholding research, and general interest in testing, the team moved forward with using -16dB, -18dB, and -20dB threshold values. While adaptive thresholding could provide a more dynamic thresholding approach, we suggest more research on Otsu's method in future work, as testing and validation with Otsu's threshold did not yield optimal results.

K-Means Clustering for classifying the values:

Using K-Means clustering (k=3), radar backscatter dB values were divided into three groups: dry land, partially flooded, and flooded. The system does not use preset thresholds; instead, it groups similar dB values according to their natural distribution. This is particularly helpful for flood analysis because places covered in water have a different radar signal reflection than dry or semi-wet surfaces. Flooded (lowest dB values <= -18), Partially Flooded (mid dB values > -18 and < -16), and Dry Land (highest dB values >= -16) are represented by the colors blue, green, and orange, respectively, in the histogram that displays the clustering output. These categories show each type of terrain's physical scattering characteristics.

More objective mapping of the flood condition was made possible by the K-Means' ability to detect minute variations in backscatter intensity. The density and distribution of each class are clearly depicted in the histogram graph, where Dry Land reflects more radar energy (right side of the graph) and Flooded regions show the strongest signal absorption (far left). The flood detection model's scalability and adaptability are improved by this unsupervised learning technique, which eliminates the need for manual threshold calibration and makes it efficient across a range of time periods and geographical locations.

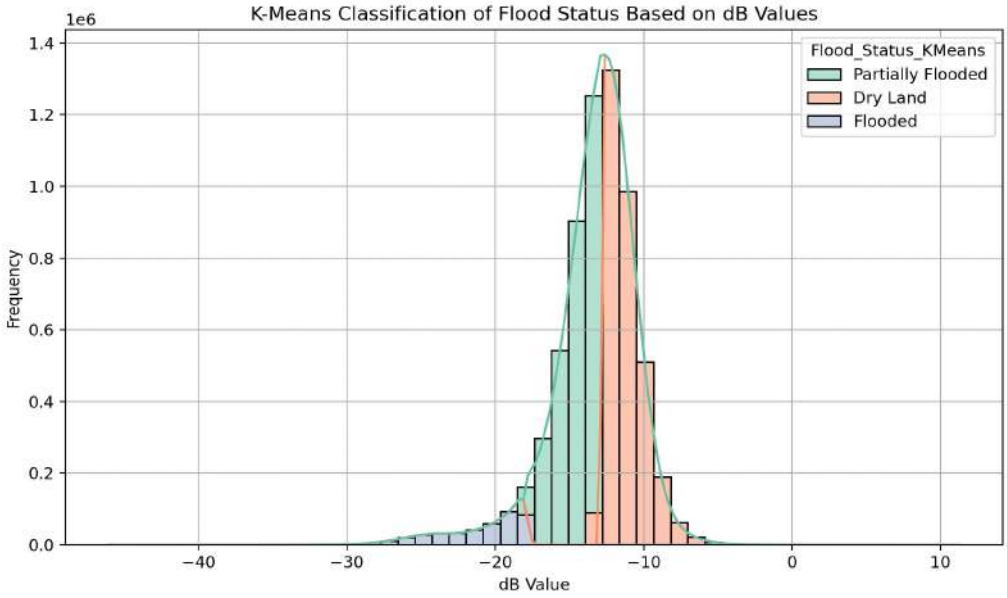

Filtering Refinement:

After the initial flood extent has been created using thresholding methods, we further refine the flood extent model using several conditions based on the pixel values within a flood polygon. These conditions include the average change of the pixel values within the flooded polygon from pre- and post-flood values, the size of the flooded polygon, and the average slope of the flooded polygon. Using these three logical conditions, we filter out polygons that don't meet all of the selected criteria.

The average change of pixel values indicates the measure of change for that flooded area. If the average change is low, it could indicate a false positive, as seen in areas surrounding rivers. Because the initial flood model returns all possible flooded areas, it often returns small polygons; the logical condition filtering based on size eliminates those small polygons that do not meet at least 1 acre. Lastly, we used the DEM to calculate the average slope of a defined flood polygon. If the average slope is greater than 5 degrees, it does not meet the logical condition because steeper sloped areas facilitate faster flood runoff.

4.1.2 Analysis

Geospatial Data Processing:

The project involves processing large geospatial datasets (Sentinel-1 SAR images) using Python-based libraries such as Rasterio and Geopandas. The analysis includes:

- Conversion of TIFF files into structured data frames.
- Normalization and speckle noise reduction using Lee filters.
- Generating flood extent polygons using QGIS and ArcGIS for visualization and analysis.
- Combining multiple pre- and post-flood images to create composite flood maps.

Model Tuning and Optimization:

- The analysis involves tuning the thresholding and classification algorithms to maximize detection accuracy, including:
    - Adjusting decibel thresholds based on terrain type and land cover.

- Fine-tuning Otsu's method using different weightings for water and land surfaces.
- Improving classification accuracy by incorporating DEM (Digital Elevation Model) data to reduce false positives from topographical variation.

Initial flood extent:

The initial flood extent is mapped by classifying and isolating post-flood image pixels that meet the water threshold, which did not previously meet the water threshold in pre-flood images. Using a threshold of -18, for example, the model would filter out pixel values that had an average pre-flood value of less than -18 dB, indicating it was already water, and eliminate pixels whose average value post-flood is above the -18 dB threshold. This would leave us with only values whose pixels were above the threshold pre-flood and now meet the flood classification.

In addition to thresholding, we filtered out pixels that had less than a 3-decibel change from the average pre-flood value to the minimum post-flood value. We used the minimum post-flood value to capture the greatest change from pre-flood to post-flood. This filtering step was used to capture only pixels that had significant change, whereas pixel values with minimal change (-1 dB) might not be indicative of a major event such as flooding. While this value of choice could be studied further, we found that this reduced the noise in our flood extent model and further increased our accuracy in testing.

$$\Delta = min_{dB\ post} - \sigma_{dB\ pre}$$

Once the possible flooded pixels are classified, flood polygons are created from the resulting overlapping pixels or pixels that touch one another. We then gather the pixel information from each polygon to aid in further refinement of the flood extent and implementation of the fuzzy logic.

Figure 6: Example Initial Flood Extent Generation (16 dB threshold)

Logical Conditions:

Backscatter change:

The average pixel backscatter values from each polygon are used to calculate the difference between pre-flood and post-flood states:

$$\sigma\Delta_{dB} = \sigma_{dB\ post} - \sigma_{dB\ pre}$$

A decrease in backscatter values indicates water accumulation, which helps in identifying flood-affected areas. A significant decrease (e.g., more than 5 dB) suggests the presence of standing water. We calculate the average change in each polygon to test the logical condition:

$$logical\ condtion\ 1: \sigma\Delta_{dB\ polygon} > 5$$

Flood size:

We measure the size of the flooded polygon by computing the area of each polygon. Using the calculated areas, we test the logical condition:

$$logical\ condtion\ 2: area_{\ polygon} \geq 2acres$$

Average slope:

Using the DEM, we calculate the slope of each pixel and take the average slope of the classified flood polygon to test the logical condition:

$$logical\ condtion\ 3: \sigma_{slope\ polygon} < 5$$

Using the above logical conditions, if an initial flood polygon does not meet all of the three, it is eliminated from the flood model.

Figure 7: Example Flood Extent After Filter (16dB threshold)

Using the described methods above, a flood extent was generated for each of the decibel thresholds, -16dB, -18dB, and -20dB, shown below.

Figure 8: Generated Flood Extent -16dB Threshold

Figure 9: Generated Flood Extent -18dB Threshold

Figure 10: Generated Flood Extent -20dB Threshold

4.1.3 Risks and Planned Mitigations

Cloud cover and radar noise:

While Sentinel-1 SAR data is designed to penetrate cloud cover and operate under all-weather conditions, radar noise from atmospheric interference and surface roughness can still reduce accuracy. Speckle noise, caused by the coherent nature of SAR signals, introduces grainy patterns that can obscure water boundaries. Speckle filtering methods, such as the Lee filter, are applied to minimize this noise while preserving important spatial details.

Mixed land cover misclassification:

Urban areas, vegetated regions, and wet soil can exhibit backscatter values similar to those of water surfaces, leading to misclassification. For example, urban surfaces reflect signals more strongly, while dense vegetation can mask underlying water. Combining VH/VV ratio analysis and adaptive thresholding could help improve the separation between water and non-water surfaces by accounting for differences in scattering behavior under different terrain conditions.

Data quality issues:

Sentinel-1 data can have acquisition gaps due to satellite orbit coverage, sensor limitations, or corrupted data transmission, resulting in incomplete flood maps. Temporal gaps between acquisitions may also lead to missed flood events. Integrating Sentinel-1 with Sentinel-2 optical data or using additional SAR sources (like RADARSAT) helps fill these gaps, improving flood detection consistency and enhancing spatial coverage.

Section 5: Testing and Validation

5.1 Testing and Validation

When testing and validating the model, the team extended the algorithm to a new AOI on Puerto Rico's coast slightly west of the first AOI. After applying the algorithm to the new AOI, we used several external data sets to validate the flood model by calculating the intersection between the generated flood extent and the validation flood extent.

5.1.1 Testing

To test the flood classification, we implemented the original modeling process on a second area of interest (AOI) in addition to the defined AOI in section 3.1. Since the model was built using this specific AOI as a case study, we wanted to ensure the workflow produced similar results in a different area. Similar to our first AOI, we pulled 3 pre-flood images and 2 post-flood images within the same dates described in the data context in section 3.3. The images below show the pre- and post-flood VH image depiction of the selected second area of interest, with a red box highlighting a portion of the map that will be the focus of further model discussion.

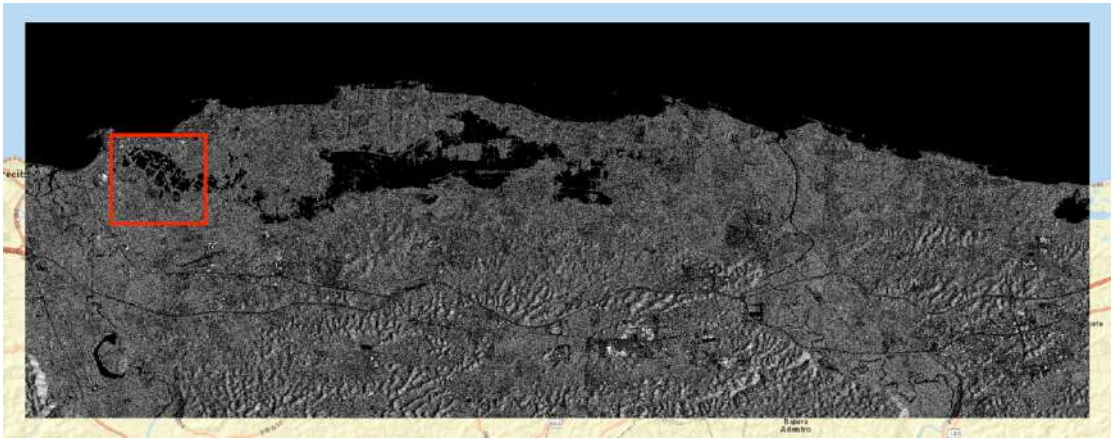

Figure 11: AOI 2 Pre-Flood VH

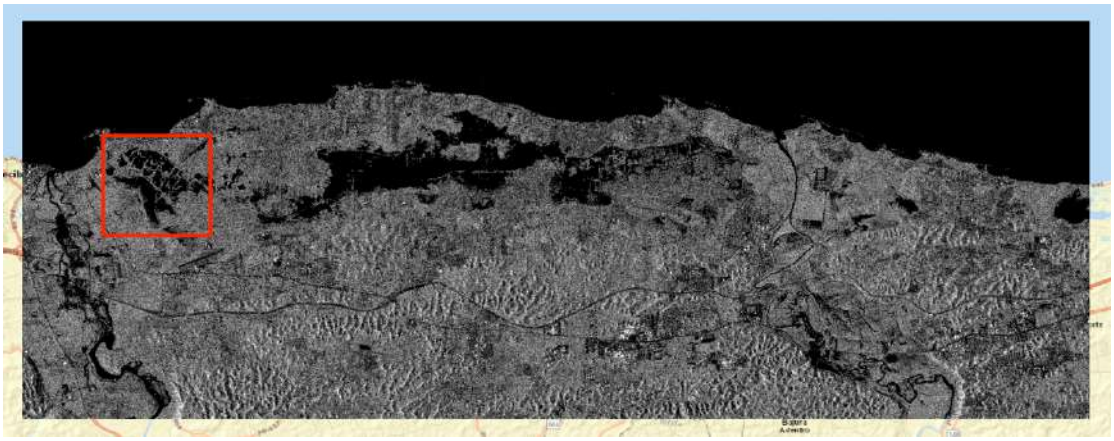

Figure 12: AOI 2 Post-Flood VH

Using our flood extent model, we applied the mapping techniques and logical filtering to create a proposed flood extent shape. The model was calculated using each of the threshold test values, -16dB, -18dB, and -20dB. We can see the differences in the pre- and post-flood images compared to the estimated flood extent (-16dB in this example) in the images below. The first figure, 13, depicts the entire flood extent, and the second figure, 14,

highlights the change from pre-flood to post-flood with the flood extent overlay in the red-boxed area from Figures 11 and 12. This comparison gives insight into the model and how it uses change detection to map floods.

Figure 13: Flood Extent Map for AOI2 -16dB Threshold

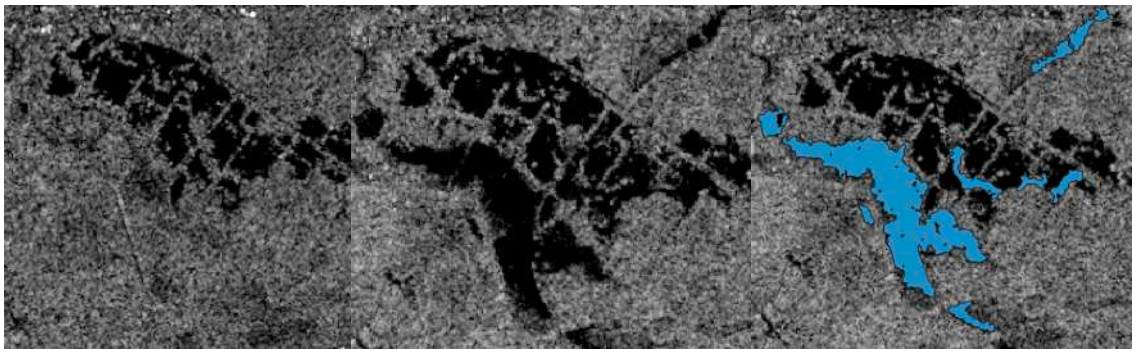

Figure 14: Pre-Flood, Post-Flood, and Flood Extent Overlay

In addition to Figure 13, the following images depict the generated flood extents for the -18dB and -20dB thresholds.

Figure 15: Flood Extent Map for AOI2 -18dB Threshold

Figure 16: Flood Extent Map for AOI2 -20dB Threshold

5.1.2 Validation

To evaluate the performance of the flood classification model, identifying accurate sources of validation data was a top priority for our team. As the flooding event of interest for developing and testing the model was Hurricane Maria, we considered sources of labeled flood data for this event for use as validation data. A review of potential validation data sources revealed that labeled flood data for Hurricane Maria, or for other flooding events in Puerto Rico, was scarce. Ultimately, two sources of validation data were chosen, each with distinct advantages and drawbacks.

The validation involved measuring the area of our generated flood extent that overlapped with the validation data flood extents and measuring the percentage of validation data that was identified with our model. This process of validation is described in the equation:

$$\%validation\ flood\ covered = \frac{intersection\ area}{validation\ flood\ area}$$

Global Flood Monitoring (GFM) Portal:

The first validation dataset selected was labeled flood data for Hurricane Maria obtained from the Global Flood Monitoring (GFM) Portal, a service provided by Copernicus. Copernicus GFM data is generated using Sentinel-1 satellite imagery, the same imagery used in our flood detection model. As such, the imagery is downloadable in raster format with a labeled flood layer. The GFM flood data is generated through a combination of three separate flood detection algorithms. Thus, a potentially high degree of error can be expected in the data. For this reason, our team did not treat the GFM data as if it were a source of ground truth when validating our flood classification model. Rather, the GFM data was used to understand how our model compared to pre-established flood detection models in terms of accuracy.

Despite its lack of ground truth due to the flood extent being generated by algorithms, similar to what we are doing in this research, we applied the validation methodology with the GFM flood extent and the combined areas of interest at each generated flood extent threshold level, -16dB, -18dB, and -20dB.

Applying the validation methods, our generated flood extent covered 30%, 40%, and 41% of the GFM flood extent for each threshold level, -16dB, -18dB, and -20dB, respectively.

Figure 17: Example Imagery of GFM Model (red) Overlayed on Generated Flood Extent (-16dB Threshold)

While these values are low, they are not accurate reflections of our flood model accuracy due to the different algorithms used to generate each flood extent and the lack of ground truth behind the GFM. Understanding the lack of ground truth behind the GFM model, the team used a second validation data set composed of aerial images post-Hurricane Maria.

National Geodetic Survey (NGS) Aerial Images:

The second validation dataset that was selected was aerial imagery made available by the National Geodetic Survey (NGS). In the aftermath of Hurricane Maria, from September 22nd to September 26th, 2017, the NGS conducted flights over Puerto Rico during which imagery was captured using specialized remote-sensing cameras to assess damages. This imagery is available for download in raster format, but unlike the GFM data, it does not include any flood labeling.

To use this NGS imagery to validate our model, our team manually created flood polygons to cover visibly flooded areas by comparing the imagery to a pre-flood basemap [Fig. 18]. The NGS imagery was much better suited for such a task than satellite-generated imagery, as the resolution of aerial imagery far exceeds that of satellite imagery. The downside of creating a validation set in this way is the potential for human error that is inherent when images are manually analyzed. On the other hand, the advantage of such a validation set is that it provides a rare source of ground-truth data that is not algorithm-based for model validation.

For this task, 2 team members manually created flood polygons using the aerial images independently of one another. Once the independent flood polygons were generated, the flood extents were merged to create a single validation flood extent map for each of the areas of interest studied.

Figure 18: Pre-Flood Base Map, Post-Flood Aerial Image, Validation Polygon

After the validation flood extent polygons were created, the validation calculation was applied to each of the generated flood extents within each area of interest. The first area of interest covered 62%, 56%, and 37% of the -16dB, -18dB, and -20dB generated flood extents, respectively, while the second AOI covered 71%, 55%, and 33% for each generated flood extent. Assuming the decrease in decibel value thresholding from -16dB to -20dB becomes more restrictive in its flood classification, it is not surprising to see less flood overlap due to the selectiveness of a lower threshold. The figure below depicts the same target area as in Figure 13, with the generated flood overlap.

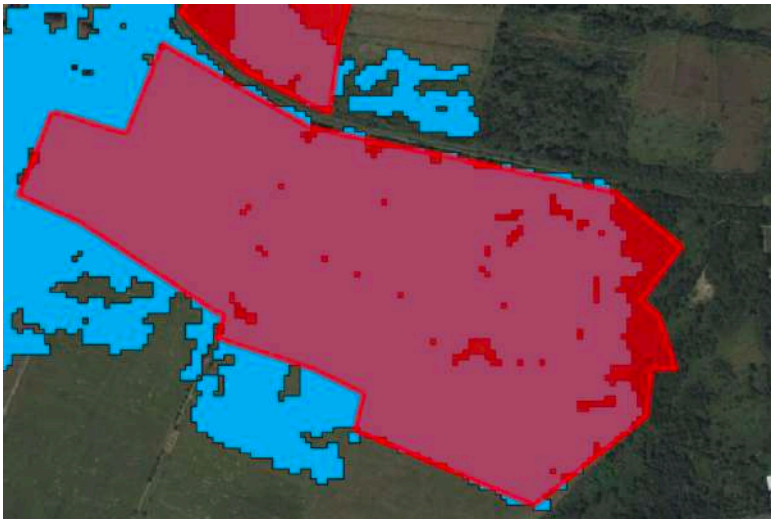

Figure 19: Hand-drawn Flood Extent (red) overlayed on Generated Flood Polygon (blue)

While the NGS data provided some ground truth and greater accuracy in the validation of the flood model, the aerial images were captured 2 days post-hurricane, while our model captures Sentinel-1 data immediately after the flood. Thus, when comparing our results to the manually created flood polygons for the NGS data, it is important to consider the time discrepancy in data collection to understand why certain areas determined by our model to be flooded may not have been covered by the NGS data polygons. With the data collection delay in mind, and no other validation data to support our generated flood extents, it's possible that our model may have a higher degree of accuracy than what was computed using the aerial image flood extents.

Section 6: Findings

Throughout this project, the team was able to create a successful flood extent boundary methodology using Sentinel-1 VH decibel imagery. Our method followed a simple and understandable logic, which was built on the foundation of change detection. By measuring and understanding the change in decibel values from pre-flood to post-flood and applying thresholding techniques, we were able to segment portions of our areas of interest that indicated potential flooding. After identifying potential flood areas, we were able to apply research-based flood indicators such as area and slope to further refine our model, which led us to a 60-70% coverage rate using our validation data.

While there are many flood extent boundary techniques that the team researched, this seemingly simple method is the foundation of understanding the change of the Earth's surface characteristics after flood disasters. When the team was gathering insight on VH decibel values, it was consistently noted that smooth water surfaces had lower decibel values compared to dry land. In particular, we found that water or flooded areas had decibel values ranging from -20 to -18, partially flooded areas from -18 to -16, and urban dry land to have decibel values typically

above -16. Throughout the implementation of our model, we tested a range of these values to look at the sensitivity of these particular thresholds in classifying flooded areas.

In general, testing the model at each threshold level of -20dB, -18dB, and -16dB gave similar yet varying results. As the threshold level decreased from -16 to -20, the model became more restrictive as the water classification threshold was more selective for those lower decibel values. On the other hand, increasing the threshold to include partially flooded areas with a threshold of -16dB was generally less restrictive and increased our flood extent boundary area in both areas of interest studied. This is shown by the figure below, which represents the flood extent boundaries for each decibel threshold. Red represents -20dB, green -18dB, and blue -16dB.

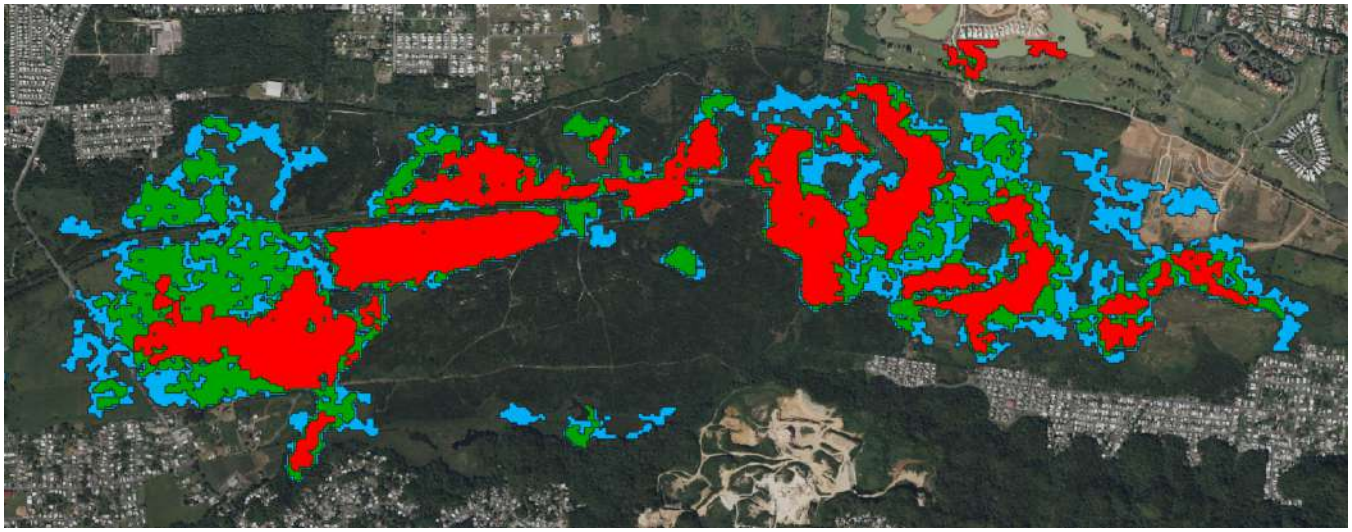

Figure 20: Flood Extent Difference Between Thresholds

After testing the various thresholds, we validated the extent of the flood model using our hand-drawn polygons from the NGS aerial images. Through this validation, we found that our -16dB threshold had the highest coverage, where 62% and 71% of areas 1 and 2, respectively, were classified by our model. We found that each decrease of our threshold from -16dB to -18dB and from -18dB to -20dB returned a lower accuracy when compared to the validation data. While we also tested our model using the adaptive thresholding of Otsu's method (-15.42dB), this threshold returned an even smaller accuracy rate, similar to the values seen by using a -20dB threshold. Because of this, we suggest further research and testing using Otsu's method or using the partially flooded threshold value of -16dB.

Through our validation process, we used two very different sources to measure accuracy. The NGS aerial imagery was the closest to ground truth, while the GFM model was an algorithm-based flood extent model. Of the total area mapped by each flood extent, there was only ~14% overlap. This difference is particularly interesting because, if we treat the aerial imagery as ground truth, this suggests a significant increase in flood model accuracy using the methods described in this paper.

Section 7: Summary

This capstone project focused on developing an automated system to detect and map post-storm flooding in Puerto Rico using Sentinel-1 Synthetic Aperture Radar (SAR) imagery. Given the region's vulnerability to hurricanes and the limitations of optical satellite imagery in post-storm conditions, SAR was selected for its cloud-penetrating

capability and reliability under adverse weather. The project's goal was to generate accurate, GIS-compatible flood extent shapefiles to support rapid disaster response and long-term resilience planning.

The flood detection pipeline leveraged change detection techniques by comparing SAR images captured before and after Hurricane Maria in 2017. After preprocessing the imagery to ensure calibration consistency and reduce noise, the team applied decibel-based thresholding at -16 dB to -20 dB to isolate flooded regions. Otsu's adaptive thresholding method was also tested to automate classification based on the distribution of backscatter values, helping to identify areas likely affected by surface water accumulation.
To improve classification accuracy and reduce misclassifications, logical refinements were incorporated. These included filters based on terrain slope (using Digital Elevation Model data) and minimum polygon area to exclude unlikely or noisy detections. One important insight during testing was that Otsu's method tended to underestimate flood extent, with thresholds differing by an average of -0.70 dB compared to manually validated benchmarks. This suggests that future versions of the system could benefit from adaptive calibration tuned to specific terrain or storm conditions.

Final outputs were validated against aerial imagery from NOAA and compared with flood maps from the Global Flood Monitoring Portal. The results showed a classification accuracy of approximately 60% to 70%. While the model occasionally overestimated flooding in vegetated or urban areas, the pipeline proved effective and scalable. This project establishes a strong foundation for future enhancements, such as integrating Sentinel-2 optical imagery, real-time flood monitoring, and expansion to other disaster-prone regions.

Section 8: Future Work

Future work to build on the work done in this project could center on one of several key aspects. One aspect of this project that future research could improve upon is the accuracy of the validation dataset. In the case of this project, labeled flood data used for model assessment and tuning was taken from two sources, one of which was algorithm-generated by another flood detection algorithm. The other source consisted of unlabeled imagery that required visual flood detection by our team. Each of these data sources has a high potential for error and various data biases. Ultimately, biases in the labeled flood validation data, such as human error or algorithmic bias, can result in biases in the flood detection model that is tuned to fit this data.

Under ideal circumstances, the flood detection model would be trained on hard, ground-truth flood data based on measurements and other data collected on the scene. Future research could seek to improve upon the validation data used in this project by attempting to identify other sources of labeled flood data or improving upon the methods used to identify flooding from the NGS post-hurricane aerial imagery data. Future research could also seek to address possible biases created by time disparities between the input imagery used in the model and the validation data. On a broader level, additional research could be conducted to improve upon other flood detection methods and flood reporting on the ground in the aftermath of flood disasters. In the process of searching for validation datasets, the lack of any kind of ground-level flood data based on physical assessments for Hurricane Maria revealed the potential need for improvement of flood reporting mechanisms.

An additional aspect of this project that future research could focus on is the project scope. In the case of this project, model tuning and testing were conducted only on a limited portion of Puerto Rico for a singular flood event, Hurricane Maria in 2017. The large amount of computing resources necessary for working with geospatial data was partially responsible for why the scope of the project was kept limited. Future research could focus on applying the flood detection model used in this project to other flooding events, both in Puerto Rico and in other

regions. A comparison of model performance across different regions and events may reveal a need for separate model creation depending on locality or flooding event type.

Another good opportunity for future work in this area would be to incorporate other types of imagery into the current model. Due to the scope and limited time, the team focused on implementation with VH decibel values. While we gathered VV decibel values in our tiffs, we primarily relied on the VH values for the initial iteration, which left no time to explore the incorporation of the VV values collected. During our research, we found that the combination of these values and calculating the VH/VV ratio could give even greater insight than VH values alone. Specifically, that water surfaces typically have a lower VH/VV ratio, and higher values of this ratio are observed in more vegetated or urban areas.

In addition to incorporating the VV values into the current algorithm, the use of other satellite imagery in flood classification can be explored, such as using Sentinel-2 optical imagery. An algorithm using solely Sentinel-2 imagery or a combination of Sentinel-1 and 2 could lead to both an increased accuracy in flood extent modeling and a faster time for flood extent generation. Because there exists a time delay in receiving satellite imagery due to the orbit schedules of Sentinel-1 and Sentinel-2, it's possible that immediate post-flood imagery may not be available when relying on one particular satellite. The future growth of rapid flood extent generation using satellite imagery may be more robust with a combination of models: one based on Sentinel-1 imagery, another on Sentinel-2, and a third exploring the combination of the satellite images.

Finally, we worked on improving the code and workflow of our current flood extent generation, but the process of deploying the model could be improved in terms of speed and ease of use for non-technical users. Despite the success of this project, it's clear that there is a lot of room for growth in generating accurate, rapid flood extent shape files. Even when comparing other methods, such as the GFM, to the aerial images, only 14% of the total area overlapped, proving the need for continued research. While this project just scratched the surface of flood extent modeling, it provides a clear understanding and foundation for future improved modeling.

This page intentionally left blank

Appendix

Appendix A: Domain Background

Client Overview: Puerto Rico Science, Technology, and Research Trust

Figure 21: Puerto Rico Science, Technology and Research Trust [13]

The Puerto Rico Science, Technology, and Research Trust (PRSTRT) [13, Fig. 21] is a nonprofit organization founded in 2004 under Public Law 214 to drive Puerto Rico's growth through innovation, science, and public health initiatives. With a mission to transform Puerto Rico into a globally recognized innovation hub, the Trust invests in research, entrepreneurship, technology commercialization, and economic resilience.

Through its Caribbean Center for Rising Seas (CCRS) initiative, PRSTRT is actively addressing flood resilience challenges across Puerto Rico and the broader Caribbean region. CCRS focuses on updating flood hazard mapping, promoting climate-resilient infrastructure, and enabling data-driven disaster response planning.

To support its mission, the Puerto Rico Science, Technology, and Research Trust, through the Caribbean Center for Rising Seas (CCRS), partners with technology-driven organizations that can operationalize flood data into actionable insights. One such collaborator is HighTide Intelligence, an environmental services company specializing in flood risk assessment and adaptation, which has been a core part of the client's team alongside members of CCRS.

As a Certified B Corporation, HighTide Intelligence leverages remote sensing, geospatial analytics, and machine learning to deliver high-precision, real-time flood insights that support policymakers, emergency responders, and communities. Founded in 2019 and based in Florida, HighTide collaborates with agencies and research institutions across Florida and the Caribbean to enhance disaster preparedness and long-term planning.

Its flagship platform, Arkly, provides property-level flood risk evaluations by integrating satellite imagery, hydrological modeling, and predictive analytics. Arkly helps users assess flood exposure, compare mitigation

strategies, and generate actionable outputs, making it a key technology in bridging data and decision-making for resilient urban planning.

Project Relevance

Building on the Puerto Rico Science, Technology, and Research Trust's broader mission to enhance disaster resilience and scientific innovation, this project directly supports the development of rapid, reliable flood detection tools tailored for Puerto Rico. Recognizing the need for near-real-time flood mapping solutions, the Trust, through collaboration with partners such as HighTide Intelligence and Arkly, has prioritized the advancement of remote sensing applications for flood risk assessment.

This project focuses on creating an automated processing pipeline that uses Sentinel-1 Synthetic Aperture Radar (SAR) data to detect flood extents accurately, even under challenging weather conditions. By leveraging the strengths of SAR imagery, particularly its ability to penetrate cloud cover and capture surface water changes, we can provide critical flood information quickly after storm events.

Our approach aims to bridge the gap between data acquisition and actionable insight. Through thresholding methods and geospatial processing techniques, flood extent maps are generated in GIS-compatible shapefile formats, allowing easy integration with emergency management workflows. This output equips disaster response teams, planners, and policymakers with the tools needed to make informed decisions rapidly during flood emergencies.

By automating key steps such as data download, preprocessing, flood detection, and shapefile creation, the project reduces manual intervention and improves operational scalability. In doing so, it aligns with the Trust's long-term vision of fostering innovation-driven, technology-enabled resilience strategies across the region.

Ultimately, this project provides the foundational capability to streamline flood mapping processes, enhance early warning systems, and support broader climate adaptation efforts, strengthening Puerto Rico's position as a leader in science-based disaster resilience.

Flood Risk in Puerto Rico and the Importance of Flood Extent Mapping

Figure 22: Hurricane damage in Puerto Rico following Hurricane Maria [14]

Puerto Rico faces a high risk of flooding due to its geographical location, climate conditions, and rapid urban expansion into flood-prone areas. The island is frequently impacted by hurricanes [14, Fig. 22], extreme rainfall events, and coastal storm surges, leading to infrastructure damage, economic losses, and displacement of communities. The steep terrain, aging drainage systems, and shifting climate patterns further contribute to widespread flood vulnerability.

Traditional flood risk assessments rely on historical data and hydrological models, but these approaches often struggle to capture real-time flood dynamics or provide timely predictions. To address these challenges, modern flood detection methods now incorporate remote sensing technologies and machine learning-driven flood mapping. By leveraging satellite imagery and automated classification models, these advanced techniques improve the accuracy and speed of flood risk assessments, enabling quicker response times and more effective mitigation strategies.

While traditional methods like aerial surveys and ground-based sensors offer valuable data, they are often slow, costly, and geographically limited. Satellite imagery, particularly from radar satellites like Sentinel-1, offers a faster, more scalable solution by detecting floods in near real-time, even through cloud cover.

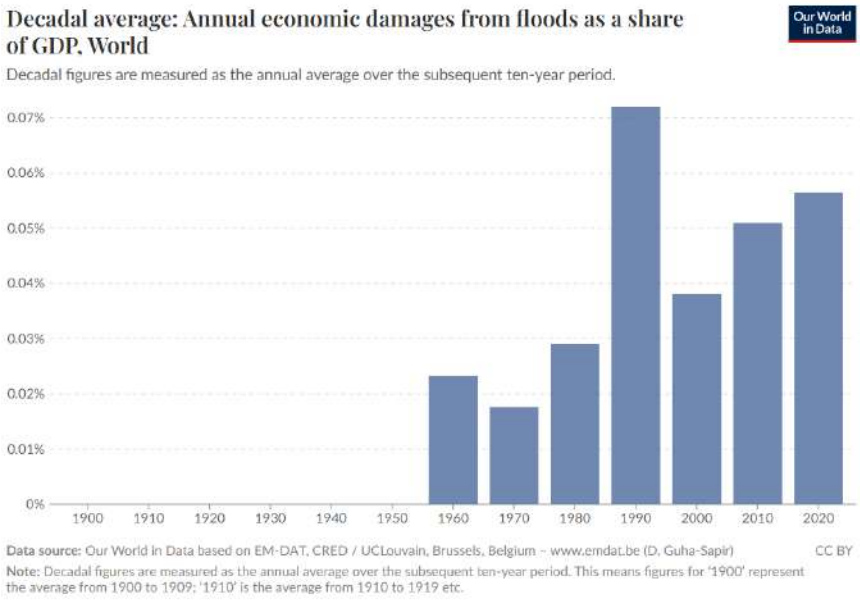

Figure 23: Annual global economic damages from floods, decadal average. [15]

Explaining the Problem Space on a Broader Scale

The problem posed by the Puerto Rico Science, Technology, and Research Trust is not unique and is one that has already been explored by a variety of organizations. More broadly, the scope of this project can be categorized under the topic of flood mapping using satellite imagery data. Flooding is one of the most prevalent and destructive natural disasters globally, annually causing billions of dollars in damage and having a tremendous impact on human populations. As illustrated in [15, Fig. 23], flood damage cost as a share of GDP has seen a steadily increasing trend. Emergency management teams, government agencies, and humanitarian groups across the globe all play a significant role in addressing flooding disasters to provide aid to the affected and rebuild damaged infrastructure. The first step taken by these organizations is usually to identify affected areas to most optimally deploy resources. In the wake of a flood-related disaster, this task can often pose a significant challenge.

One solution for this problem that has become increasingly widespread is the use of satellite imagery data to detect flooding.

Traditional flood mapping methods, such as aerial imaging, hydrological modeling, and in-situ sensor networks, are often costly, time-intensive, and geographically limited. These approaches rely heavily on manual data collection and processing, leading to delays in flood assessments during extreme weather events. In contrast, satellite-based remote sensing enables near-real-time flood detection at a large scale. For these reasons, the Puerto Rico Science, Technology, and Research Trust is interested in focused on utilizing this specific method of flood detection.

Problem Overview

The project problem posed by the Puerto Rico Science, Technology, and Research Trust has several key components, each of which must be addressed to cover the entire problem scope. The first of these components is the data source. Because the area of interest of this problem is Puerto Rico, sources of satellite data must contain data from this region. Additionally, because the company is seeking to provide real-time flood extent mapping, the source of the data must update regularly with data that is as recent as possible. Potential sources of satellite imagery data that were provided by the Puerto Rico Science, Technology, and Research Trust for consideration included NASA's Disaster Response Coordination System (DRCS) imagery from Tropical Storm Ernesto, open-source datasets from the U.S. Geological Service (USGS), and other sources of historical flood extent data. Among potential sources of such historical flood extent data are NASA Landsat data and Copernicus Sentinel-1 and Sentinel-2 data. Because Sentinel-1 data utilizes synthetic aperture radar (SAR) satellite imagery, it is this source that is of greatest interest to this project.

The advantage provided by synthetic aperture radar (SAR) satellite imagery, such as that generated by Sentinel-1, is its ability to provide continuous, high-resolution imaging, unaffected by weather conditions or cloud cover. Unlike optical satellites that rely on visible light, SAR uses microwave signals that penetrate atmospheric interference, enabling precise detection of surface water changes. Satellites that utilize optical sensing lack this unique advantage, making SAR an invaluable tool for capturing both gradual and extreme flood events in real time.

Another component of the problem is the selection of flood detection methods. Once a data source is selected, flood detection typically requires the use of multiple SAR satellite image data sets for any given area of interest. One of these data sets is generally a baseline dataset of pre-flood data, whereas another dataset is the dataset of a selected flood for mapping. In the case of Sentinel-1 SAR images, imagery can be obtained with either VV or VH polarization bands. While VH imagery is oftentimes more useful for flood detection than VV imagery, both imagery types may present certain advantages or disadvantages depending on factors such as terrain or vegetation in the area of interest. To detect flooding, a variety of machine learning techniques and thresholding methods can be applied to backscatter values, which are essentially the pixel values generated by SAR imaging. Prior research on the topic suggests that ensemble methods employing a combination of multiple thresholding and machine learning techniques may be the most effective at flood detection.

The final component of the problem is generating a user-friendly output that allows interested parties to readily and efficiently utilize flood detection results. The Puerto Rico Science, Technology, and Research Trust has indicated that their desired output should be in a shapefile format. This format is compatible with GIS software and allows detected flooding to be readily overlayed with other layers for user-friendly flood identification.

Additionally, the creation of an API that allows users to easily input Sentinel-1 imagery and obtain shapefile results as simply as possible and without requiring a technical understanding of the underlying processes is a requirement for this project. This development will streamline the flood detection process for interested parties to facilitate more effective flood disaster response and detection.

Appendix B: Glossary

Term	Definition
Synthetic Aperture Radar (SAR)	A Satellite-based remote sensing method that uses microwave signals to create high-resolution images, enabling all-weather flood detection.
VV/VH Polarization	SAR imaging bands used to distinguish water bodies from land surfaces, improving the accuracy of flood extent classification. VH - vertical transmit, horizontal receive VV - vertical transmit vertical receive
Shapefile (GIS)	A geospatial data format used for storing vector-based geographic information, widely applied in flood mapping and disaster response planning.
Floodplain Zoning	A land classification system that designates areas based on flood risk levels, aiding municipalities in development regulations and infrastructure planning.
Hydrological Modeling	A predictive simulation technique that analyzes water flow, precipitation impacts, and flood behavior under various environmental conditions.
AOI	Area of interest
Backscatter	Measure of wave strength received from satellite
Radiometric	Properties of radio electromagnetic radiation
Orthorectification	Correction for terrain and geometric errors
GeoTiff	Image type data file with geometric coordinate reference

Table 1: Glossary Table

Appendix C: GitHub Repository

Overview (READ.me)

To run the flood extent generation, we first need to pick the location of interest and identify boundaries for "cells" or shapes to load in the API data.

- For our first iteration, we created a grid on QGIS
- Need to ensure each area of interest, or cell, is small enough to allow image download resolution to be 10m per pixel
- A guide for possible grid values and the corresponding boundary points can be found in the puertorico_grid Excel sheet

After boundaries for cells or areas of interest are defined, we use the process_api_connection.py script and dem_process_api.py to pull the data. The process Api file will pull the VV and VH values of the pixels in defined cells. The DEM process API file will pull the DEM values for the specified cell to be used in slope calculation

- Ensure Copernicus credentials are valid
- Pull 3 pre-flood images and 2 post-flood images
- The current process will pull both VH and VV (VH in band 0 and VV in band 1)
- NOTE: these tiffs are not optimized for visual use since we don't have RGB bands, only used for data (i.e., it won't create the black and white images)
- This will create all the tiffs for analysis in different folders that currently need to be manually renamed and moved to the appropriate folders.
- See more notes in the Python script for usage.

Currently, all tiffs used in our analysis are in the geo_tiffs folder with the naming convention pre/postfloodimagenumber_cellnumber (ex, postflood1_01.tiff), where the 1 after pos- flood indicates it is the first pre-flood image, and 01 represents the cell.

After all tiffs have been downloaded, we use the geotiff_to_csv.py script to generate a CSV of all points, their coordinates, and the corresponding VH/VV value. Band [0] will grab the VH values, and band [1] will grab the VV values. See more notation in the geotiff_to_csv.py for detailed info. The script currently creates a CSV per cell. The CSVs are located in the geotiff_csvs folder and are labeled by cell and value they contain (either vh or vv)

Similar to the VV/VH GeoTIFF, we also convert the slope GeoTIFF to CSVs. After running the geotiff_to_csv.py for the DEM tiffs, we use the slope.py file to calculate the slope values using the DEM values in our CSV. The resulting slope values are saved in a CSV for later use.

The initial_flood_extent.py is 1 of the 2 key scripts used to run our model. It first merges all CSVs of the areas of interest and calculates needed metrics such as mean change. After initial calculations, the thresholding method is applied. Once the thresholding method is applied, the only pixels remaining in the data frame are pixels that might indicate possible flooding. We take these pixels and turn them into shape files where overlapping/neighboring points represent a flooded polygon. We can map this shape file to QGIS to get the current flood extent.

To prepare for the logical conditioning, we use a loop to assign points to each flood extent polygon. We do this to get the values of the points within the flooded polygon. EX. Polygon 1 contains points 1,2,3,4,5, and these are the decibel values we have/change values we have for those points.

After we finish running the initial_flood_extent.py, we have all the needed information to refine our flood extent. We then move to the 2nd key script, flood_extent_filtering.py. We gather the information on our initial flood extent and for each polygon calculate the area, mean change, and mean slope. We then apply our conditional filtering, where all three conditions (area greater than or equal to 2 acres, mean change of at least 5dB, and mean slope value below 5 degrees) must be satisfied.

Finally, we filter out polygons that do not satisfy the three logical conditions and generate the final flood extent shape file to be mapped using any GIS software.

Within GitHub, there is another branch called automation, where development to automate the current process was being conducted and tested for future development.

GitHub Repository Link

Link to Repo

GitHub Repository Contents

- Archive Folder: contains all testing and previous work
- Dem_slope_csvs Folder: contains a CSV of the DEM values for each cell
- Dem_tifs Folder: contains the GeoTIFF for each cell collected using the DEM process API
- Final_flood_extent Folder: contains all final flood extent boundaries and intermediate flood extent files
- Geo_tiffs Folder: contains all GeoTIFF and JSON files for the VV and VH values used in the analysis
- Geo_tiff_csvs Folder: contains all CSVs of values collected from the GeoTIFF
- Puertoricoshape Folder: contains a map of the mainland Puerto Rico
- Testing_shapes Folder: contains all of our testing polygons
- Visuals_all_geotiffs_single_image: contains black and white image representations of our VH and VV values
- Otsus.py: Otsus method script
- Dem_process_api.py: Script to pull DEM values
- Flood_extent_filtering.py: Script to refine the initial flood extent with logical conditions
- Geotiff_to_csv.py: Script to convert GeoTIFF to a data frame CSV
- Initial_flood_extent.py: Script that creates the initial flood extent after thresholding
- Process_api_connection.py: Script that connects to Copernicus API to pull needed decibel values (currently pulls both VH and VV values)
- Puertorico_grid_values.xls: grid composed of cells for future data pulls, including grid coordinates
- Slope.py: Script that calculates the slope using the DEM values collected
- Validation.py: Script that reads the validation polygons and our generated flood extent, and calculates the flood classification accuracy

Appendix D: Risks

Sprint 1 Risks

Risk	Description	Probability	Impact	Mitigation
Copernicus API access	Need Access to Copernicus API or files from Copernicus	Low	High	Work with the client to understand the output format of Copernicus data to begin working on algorithm and stay up to date on access
Unknow file format	File format of the data is currently unknown (jpg, GeoTIFF, etc.)	Low	Medium	Research Copernicus satellite imagery file format
Quality of Data	Data is messy and takes large amount of time to clean and grab useful information from	Medium	Medium	Get a head start on data understanding
Integration issues	Product is incompatible with user systems	Medium	High	Through product development ensure base code is readable by user systems and test often

Table 2: Sprint 1 Risks

Sprint 2 Risks

Risk	Description	Probability	Impact	Mitigation
Copernicus API connection data size	Proper resolution images (10M per pixel) are only available in small batches using Copernicus API, need images for entirety of PR	Medium	Low	Try to explore batch processing methods or create functions that will loop through a specified geometry
SAR Data Preprocessing Complexity	Sentinel-1 data requires multiple preprocessing steps (calibration, speckle filtering, terrain correction), which can be time-consuming.	Medium	Medium	Automate preprocessing during data download API options

Flood Classification Threshold Selection	Backscatter values for water vary by region and terrain, making threshold-based classification unreliable	Medium	High	Use adaptive thresholding or machine learning-based classification for improved accuracy.
Speckle Noise Affecting Classification	Sentinel-1 SAR images contain speckle noise that can reduce the accuracy of flood detection.	Low	Medium	Apply adaptive speckle filtering (e.g., Lee, Gamma-MAP) while preserving edges and important features. Use multi-temporal filtering for better results.
Memory and Processing Resource Constraints	Processing high-resolution data for multiple grid sections can strain available computing resources, potentially leading to slow processing or system crashes.	Medium	Medium	Optimize processing scripts and consider using high-performance computing (HPC) or cloud-based platforms (e.g., AWS, Google Cloud) to distribute the workload.

Table 3: Sprint 2 Risks

Sprint 3 Risks

Risk	Description	Probability	Impact	Mitigation
Limited Generalization Across Regions	A single threshold (e.g., -19.37 dB) may not work universally for different terrains and flood events	High	High	Implement adaptive thresholding or region-specific calibration using historical flood data
Interpretation of "Partially Flooded" Zone	The middle zone (e.g., -18 to -16 dB) is ambiguous and may overlap with vegetation backscatter	Medium	Medium	Consider incorporating polarization (VV/VH) ratios or temporal changes for finer classification
False Positives in Flood Detection	Certain land features (e.g., roads, wetlands) may be misclassified as floodwater due to	Medium	High/Medium	Integrate auxiliary datasets (DEM, land cover maps) to refine classification accuracy

	similar backscatter properties			
Data Storage & Processing Constraints	Large SAR image files require significant storage and computational power, slowing down processing and analysis	Low	Medium	Use cloud-based processing (e.g., Google Earth Engine, AWS) and optimize raster data storage formats
Speckle Noise Affecting Classification	Sentinel-1 SAR images contain speckle noise that can reduce the accuracy of flood detection	Low	Medium	Apply adaptive speckle filtering (e.g., Lee, Gamma-MAP) while preserving edges and important features. Use multi-temporal filtering for better results
Lack of Ground Truth / Validation Without validation	Classifications are hard to trust	High	Medium	Use publicly available flood maps (e.g., Copernicus EMS or FEMA) or compare to optical images for known flood areas
Loss of Spatial Resolution	Resampling or conversion to CSV can lose fine-grained details of the terrain	Medium	Medium	Keep original resolution when converting raster to tabular format; store pixel dimensions for reference

Table 4: Sprint 3 Risks

Sprint 4 Risks

Risk	Description	Probability	Impact	Mitigation
Interpretation of "Partially Flooded" Zone	The middle zone (e.g., -18 to -16 dB) is ambiguous and may overlap with vegetation backscatter	Medium	Medium	Consider incorporating polarization (VV/VH) ratios or temporal changes for finer classification
False Positives in Flood Detection	Certain land features (e.g.,	Medium	Medium	Integrate auxiliary datasets (DEM, land

	roads, wetlands) may be misclassified as floodwater due to similar backscatter properties			cover maps) to refine classification accuracy
Lack of Ground Truth / Validation Without validation	Classification accuracy is uncertain, as the available ground truth images were captured **four days** after the peak flooding event	High	Medium	Use publicly available flood maps (e.g., Copernicus EMS or FEMA) or compare to optical images for known flood areas
Human Error in Validation methods	Using Aerial imagery as a validation source requires us to manually generate flood polygons. These may not be 100% accurate	High	Medium	Ensure strategic creation of polygons.

Table 5: Sprint 4 Risks

Sprint 5 Risks

Risk	Description	Probability	Impact	Mitigation
Lack of Ground Truth / Validation Without validation	Classification accuracy is uncertain, as the available ground truth images were captured four days after the peak flooding event.	High	Medium	Use publicly available flood maps (e.g., Copernicus EMS or FEMA) or compare to optical images for known flood areas
Human Error in Validation methods	Using Aerial imagery as a validation source requires us to manually generate flood polygons. These may not be 100% accurate	High	Medium	Ensure strategic creation of polygons.
Slide Quality	Too much information on final slides, color contrast from words and	Low	Medium	Get and use feedback from final presentation feedback

	background, text readability			
Presentation quality	Speakers unclear or unsure of what they are speaking to. Too much or too little information. No filler words	Low	Medium	Practice sections and ensure that the story has a clear flow. All information is explicit, necessary, and makes sense to non-technical audience as much as possible

Table 6: Sprint 5 Risks

Appendix E: Agile Development

Scrum Framework Team Approach

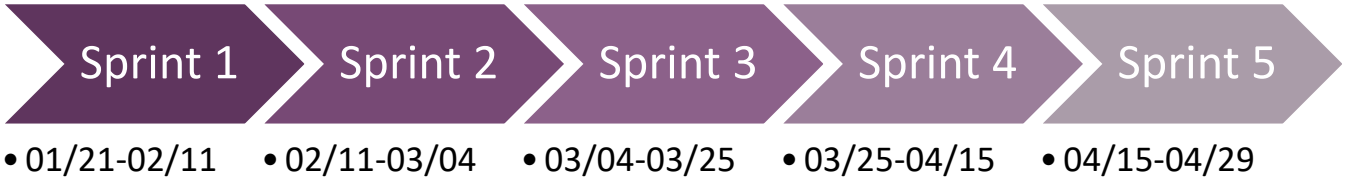

Figure 24: Sprint dates.

In addition to the primary project objectives, the team practiced using an agile framework for product development. The team adapted well to the main pillars of Agile and had scheduled daily scrum meetings on weekdays with longer team meetings, if necessary, on the weekends.

In the initial stages of the project, the team worked together to research flood detection methodology and possible data sources. As we progressed through the initial stage, we tested implementing several flood detection methodologies and used our daily scrum meetings to explore each other's findings. After gaining a better understanding of our data sources and methodology, it was crucial to balance the workload between teammates, whether it be assigning portions of the paper to be written or assigning tasks on methods through YouTrack. The nature of assigning tasks ensured that progress was being made on all aspects of the project throughout the semester.

Utilizing the agile framework helped our team stay connected through development and keep clear and open lines of communication. It allowed us to stay on top of deadlines and push through tasks on each sprint. Weekly client meetings on Fridays were especially helpful for getting client feedback and guidance as we progressed throughout the project.

Sprint 1 Lessons Learned

During Sprint 1, the team focused on data collection, preprocessing, and preliminary flood detection analysis with Sentinel-1 SAR imagery. We effectively recovered and arranged pre- and post-flood VV and VH photos, guaranteeing proper storage and accessibility for the study. Setting up QGIS and ArcGIS allowed us to view and compare changes, but interpreting SAR backscatter values proved difficult, necessitating more research and hands-on experimentation. While basic change identification was implemented, the difference analysis between pre- and post-flood photos took longer due to differences in SAR intensity values. Furthermore, dealing with huge datasets caused processing delays, prompting us to improve our workflow and investigate approaches for faster raster calculations.

The team utilized YouTrack to coordinate work, which clarified sprint goals while revealing areas for improvement in task distribution and time management. Some participants concentrated on SAR data processing, while others investigated AI/ML models for flood categorization; nonetheless, a more organized collaborative approach would have better-balanced efforts. The lack of a finished AI/ML model throughout this sprint underlined the necessity for more specific criteria for determining the best technique. Furthermore, while some team members had prior experience with GIS and remote sensing, others needed more time to learn, which reduced sprint velocity marginally. In Sprint 2, we plan to increase collaboration, refine AI model selection, and automate flood detection.

Sprint 2 Lessons Learned

During Sprint 2, the team focused on completing data collection and preprocessing of Sentinel-1 SAR satellite imagery. VV and VH images from before and after Hurricane Maria were downloaded and processed by all members of the team for the designated area of interest. This image data was then consolidated, and QGIS was used to view the data. Furthermore, the team worked to convert downloaded data into a .csv format to facilitate further analysis. A preliminary exploration of backscatter value thresholding was conducted by the team at the end of this sprint, and the team began researching potential algorithms for flood detection in preparation for sprint 3.

One of the primary challenges of this sprint was deciding how to divide tasks among team members, as sprint 2 involved tasks that were more specific than the general research-related tasks of sprint 1. In the case of the Sentinel-1 imagery retrieval, the use of a grid method where each team member was assigned particular grid squares from the overall area of interest greatly facilitated efficient data retrieval. By assigning responsibility for different portions of the data, the team also had a way of splitting up future tasks related to data processing, transformation, and analysis. The team also adapted to the new demands of the project workload by assigning unique tasks to different team members. While negotiating this division of labor was a challenging adjustment at first, it allowed team members to better concentrate their focus, and team productivity was improved.

Sprint 3 Lessons Learned

During Sprint 3, the team advanced by shifting from preprocessing to implementing core flood detection techniques. Using previously prepared pre- and post-flood Sentinel-1 SAR imagery, extracted backscatter values, converted them to decibels (dB), and consolidated the data into structured CSV files for easier analysis. We successfully implemented both Otsu's thresholding method and K-means clustering to classify flooded, partially flooded, and dry areas, which marked the transition from static thresholding to algorithm-driven decision-making. Visualizations were created using histogram analysis and spatial scatter plots to better interpret flood classifications.

The challenge in Sprint 3 was calibrating slope and decibel thresholds for accurate classification, as flood boundaries were often dependent on terrain elevations or urban reflections. The team mitigated this by incorporating DEM slope filtering and beginning the integration of fuzzy logic rules. By assigning smaller, focused tasks (e.g., flood classification tuning, slope calculation, fuzzy logic conditions), we streamlined individual responsibilities and improved parallel workflow efficiency. Validation with client feedback also ensured iterative improvement toward the end goal of generating precise flood extent shapefiles.

Additionally, automated procedures that can scale across huge datasets were developed to extract DN and dB values from numerous TIFF files. For elevation-aware filtering, gradient-based techniques were used to compute slope values. Finally, Sprint 3 was a significant stride in turning unprocessed satellite data into useful geographic flood intelligence.

Sprint 4 Lessons Learned

During Sprint 4, the team focused on refining the flood methodology and validation efforts with third-party flood extent data. To minimize missclassification areas, the team placed stricter boundaries on the initial flood extent and changed from fuzzy logic conditioning to more strict logic conditioning that required flood extent polygons to adhere to all flood rules, including minimum slope values, mean change values, and area.

The main lift for the team was validating our flood polygons, which was one of the key objectives the client gave at the beginning of the project. The team spent time searching for accurate ground truth flood polygons from Hurricane Maria, but found no such data. Despite the lack of ground truth data, we did find aerial imagery from several days after the hurricane, which allowed the team to create hand-drawn polygons of human-identified flood areas. We then used this data from several team members to validate the flood polygons generated by our model by overlaying the aerial image polygons on top of the generated flood extent.

Throughout this sprint, the team needed to keep clear communication on any model tuning and ensure the paper was kept up to date with any new additions. We were lucky to find any flood validation data, especially for our specific areas of interest, as the aerial imagery did not cover the entirety of Puerto Rico. Given the validation data we found, it was crucial to ensure minimal human error by gathering different team members' input on the boundaries of the validation flood data.
Wrapping up Sprint 4, the team successfully met all objectives that were set out at the beginning of the project and completed all development through GitHub. Additionally, members of the team worked on implementing the model in a more automated way through GitHub to be able to provide easier use in time-sensitive cases. While automation may not be complete, we thought any forward progress in this area would be a benefit to the client and future users of the product.

Sprint 5 Lessons Learned

During sprint 5, the team concentrated on completing the end-to-end flood detection pipeline, combining all created elements into a unified and repeatable process. This involved combining the results of the K-means clustering and Otsu thresholding methods, GIS mapping, and the classification thresholds, confirming uniformity over all flooded areas.

This sprint's effective creation of extensive flood extent shapefiles from thresholding, classification, and GIS mapping outputs was a major success. These were cross-checked for spatial consistency using both manual and GFM-provided validation polygons. In addition, topographic limitations were used to maintain realism by adjusting the slope and DEM filters to lower false positives in flood classification.

It also included final delivery and presentation preparation. The group ensured the GitHub repository was comprehensive and user-ready, produced visualizations, and produced thorough documentation. To communicate the technical workflow to stakeholders who were not technical, close cooperation was necessary to ensure that all slides had the same images, conclusions, and procedures.

Ultimately, all sprint objectives were accomplished. In defining realistic flood extents, the finished model performed admirably and matched both scientific assumptions and aerial photography.

References

Works Cited

[1] L. Archer *et al.*, "Current and future rainfall-driven flood risk from hurricanes in Puerto Rico under 1.5 and 2 °C climate change," *Natural Hazards and Earth System Sciences*, vol. 24, no. 2, pp. 375–396, Feb. 2024, doi: 10.5194/nhess-24-375-2024.

[2] NOAA's National Weather Service, "Major Hurricane Maria - September 20, 2017." https://www.weather.gov/sju/maria2017

[3] "Ernesto brings dangerous seas to North America's Atlantic coast," *National Environmental Satellite, Data, and Information Service*, Feb. 14, 2025. https://www.nesdis.noaa.gov/news/ernesto-brings-dangerous-seas-north-americas-atlantic-coast

[4] Climate Change Resources Inc., "Puerto Rico | Climate change resources," *Climate Change Resources* |, Jul. 08, 2023. https://climatechangeresources.org/learn-more/states/puerto-rico/

[5] HighTide Intelligence, "HighTide | Sea level rise adaptation and Flood Mitigation," *HighTide*, Dec. 17, 2024. https://hightide.ai/

[6] Nsanchez, "Caribbean Center for Rising Seas - Puerto Rico Science, Technology & Research Trust," *Puerto Rico Science, Technology & Research Trust*, Feb. 14, 2025. https://prsciencetrust.org/ccrs/

[7] "Landsat Missions," *USGS*, Feb. 07, 2025. https://www.usgs.gov/landsat-missions

[8] "Documentation - data." https://documentation.dataspace.copernicus.eu/Data.html

[9] "Synthetic Aperture Radar (SAR)," *NASA Earthdata*, Nov. 22, 2024. https://www.earthdata.nasa.gov/learn/earth-observation-data-basics/sar

[10] A Bayesian network for flood detection combining SAR imagery and ancillary data. (2016, June IEEE Journals & Magazine | IEEE Xplore. https://ieeexplore.ieee.org/document/742975

[11] Kussul, N., Shelestov, A., & Skakun, S. (2008). Grid system for flood extent extraction from satellite images. Earth Science Informatics, 1(3–4). https://doi.org/10.1007/s12145-008-0014-3

[12] Cortes, C., & Vapnik, V. (1995). Support-vector networks. Machine Learning, 20(3), 273–297. https://doi.org/10.1007/bf00994018

[13] Puerto Rico Science, Technology & Research Trust, *Annual Report 2024 – Compendio de Ciencia y Tecnología 2025*, Dec. 26, 2024. [Online]. Available: https://prsciencetrust.org/wp-content/uploads/2024/12/AR2024-Compendio-2025-12-26.pdf

[14] M. Izard-Carroll, "Damaged power lines along a road in Humacao, Puerto Rico, one of the island's hardest hit municipalities," *U.S. Army Corps of Engineers: The Longest Blackout in U.S. History – Hurricane Maria*, Sep. 2022. [Online]. Available: https://www.usace.army.mil/

[15] Our World in Data, "Total economic damages from floods as a share of GDP," dataset, based on EM-DAT, CRED/UCLouvain, Brussels, Belgium, processed by Our World in Data. Available: https://www.emdat.be

This page intentionally left blank